

UNIVERSITY OF CALIFORNIA

Radiation Laboratory  
Berkeley, California

Contract No. W-7405-eng-48

SPALLATION-FISSION COMPETITION IN HEAVIEST ELEMENTS;  
HELIUM ION INDUCED REACTIONS IN PLUTONIUM ISOTOPES

Richard A. Glass, Robert J. Carr,  
James W. Cobble, and Glenn T. Scaborg

June 1956

## **DISCLAIMER**

**This report was prepared as an account of work sponsored by an agency of the United States Government. Neither the United States Government nor any agency Thereof, nor any of their employees, makes any warranty, express or implied, or assumes any legal liability or responsibility for the accuracy, completeness, or usefulness of any information, apparatus, product, or process disclosed, or represents that its use would not infringe privately owned rights. Reference herein to any specific commercial product, process, or service by trade name, trademark, manufacturer, or otherwise does not necessarily constitute or imply its endorsement, recommendation, or favoring by the United States Government or any agency thereof. The views and opinions of authors expressed herein do not necessarily state or reflect those of the United States Government or any agency thereof.**

## **DISCLAIMER**

**Portions of this document may be illegible in electronic image products. Images are produced from the best available original document.**

- |        |                                                                                                                                                                                                                                                                                                                                                                                                                                                                                                                                                                                                                                                                                                                                                              | Page |
|--------|--------------------------------------------------------------------------------------------------------------------------------------------------------------------------------------------------------------------------------------------------------------------------------------------------------------------------------------------------------------------------------------------------------------------------------------------------------------------------------------------------------------------------------------------------------------------------------------------------------------------------------------------------------------------------------------------------------------------------------------------------------------|------|
| Fig. 1 | Diagram of successive chemical operations for the isolation of spallation and fission products from plutonium targets.                                                                                                                                                                                                                                                                                                                                                                                                                                                                                                                                                                                                                                       | 11   |
| Fig. 2 | Diagram of spallation products from $\text{Pu}^{239}$ . Compound nucleus formations is shown for convenience (although this is probably not always the case) between the helium ion and $\text{Pu}^{239}$ , which thereby states the evaporation chain from the excited $\text{Cm}^{243}$ nucleus. Points designating observed products are enclosed in squares. Arrows indicating possible reaction paths are labeled with total particles emitted from $\text{Cm}^{243}$ and (in parenthesis) energy thresholds for the reactions. Dashed arrows are employed for less probable paths. Half-lives for the products are included above the isotope symbols. The usual notation is used in which n = neutron, p = proton, f = fission, $\gamma$ = gamma ray. | 12   |
| Fig. 3 | Excitation functions for helium ion induced spallation reactions in $\text{Pu}^{238}$ .                                                                                                                                                                                                                                                                                                                                                                                                                                                                                                                                                                                                                                                                      | 17   |
| Fig. 4 | Excitation functions for helium ion induced spallation reactions in $\text{Pu}^{239}$ .                                                                                                                                                                                                                                                                                                                                                                                                                                                                                                                                                                                                                                                                      | 18   |
| Fig. 5 | Excitation functions for helium ion induced spallation reactions in $\text{Pu}^{242}$ .                                                                                                                                                                                                                                                                                                                                                                                                                                                                                                                                                                                                                                                                      | 19   |
| Fig. 6 | Yield curves for helium ion induced fission in $\text{Pu}^{238}$ for three energies: o = measured points; ● = points from reflection about the mid-point.                                                                                                                                                                                                                                                                                                                                                                                                                                                                                                                                                                                                    | 20   |
| Fig. 7 | Excitation functions for fission and summed spallation reactions in $\text{Pu}^{238}$ . The dashed line represents the percent of both fission and spallation reactions going into spallation.                                                                                                                                                                                                                                                                                                                                                                                                                                                                                                                                                               | 21   |

Fig. 8	Yield curves for helium ion induced fission in $\text{Pu}^{239}$ for ten energies. $\circ$ = measured points; $\circ$ = points from reflection about the mid-point.	Page 22
Fig. 9	Excitation functions for fission and summed spallation reactions in $\text{Pu}^{239}$ . The dashed line represents the percent of both fission and spallation going into spallation.	23
Fig. 10	Excitation functions for the total of determined helium ion induced reactions in $\text{Pu}^{238}$ and $\text{Pu}^{239}$ . Dashed lines are for theoretical reaction cross sections calculated for $r_0 = 1.5 \times 10^{-13}$ and $r_0 = 1.3 \times 10^{-13}$ by Blatt and Weisskopf (see ref. 31).	24

SPALLATION-FISSION COMPETITION IN HEAVIEST ELEMENTS;  
HELIUM ION INDUCED REACTIONS IN PLUTONIUM ISOTOPES\*Richard A. Glass, Robert J. Carr,<sup>†</sup>  
James W. Cobble,<sup>‡</sup> and Glenn T. Seaborg.Radiation Laboratory  
and Department of Chemistry and Chemical Engineering  
University of California, Berkeley, California

June 1956

## ABSTRACT

Excitation functions have been determined for the spallation and fission reactions induced in plutonium isotopes by 20 to 50 Mev helium ions. The method employed consisted of cyclotron bombardments of plutonium oxide followed by the chemical isolation and alpha or beta counting of radioactive reaction products. Formation cross sections are given where possible for the curium and americium spallation products corresponding to  $(\alpha, n)$ ,  $(\alpha, 2n)$ ,  $(\alpha, 3n)$ ,  $(\alpha, 4n)$ ,  $(\alpha, 5n)$ ,  $(\alpha, p)$ ,  $(\alpha, pn \text{ or } d)$ ,  $(\alpha, p2n \text{ or } t)$ , and  $(\alpha, p3n)$  reactions in  $\text{Pu}^{238}$ ,  $\text{Pu}^{239}$ , and  $\text{Pu}^{242}$ . Fission yield curves and fission cross sections for  $\text{Pu}^{238}$  and  $\text{Pu}^{239}$  serve to define the characteristics of the  $(\alpha, f)$  reaction for plutonium isotopes. Chemical procedures are outlined for the separation of both spallation and fission product elements in a sequence of operations performed on the entire dissolved target.

The small spallation and large fission cross sections observed indicate that fission competes successfully for most of the total reaction

\* Based in part on the Ph.D. thesis of R. A. Glass, University of California, June 1954 (also published as University of California Radiation Laboratory Unclassified Report UCRL-2560 (April 1954)) and on the Ph.D. thesis of R. J. Carr, University of California, Sept. 1956 (also to be published as a University of California Radiation Laboratory Unclassified Report UCRL-3395 (June 1956)).

† Present address, Department of Chemistry, State College of Washington Pullman, Washington

‡ Present address, Department of Chemistry, Purdue University Lafayette, Indiana.

THIS PAGE  
WAS INTENTIONALLY  
LEFT BLANK

cross section in the energy range studied. Analysis from a compound nucleus viewpoint of the cross sections for the surviving  $(\alpha, xn)$  products reveals mean  $\sigma_f/\sigma_n$  values for compound and intermediate compound nuclei from 1 to 7, the value decreasing with increasing mass number and apparently not greatly dependent on excitation energy above fission and neutron emission thresholds. The relatively high cross sections ("tails") evident in the spallation excitation functions beyond their maxima constitute evidence for processes other than compound nucleus formation, e.g., direct interaction. Even more convincing evidence for non-compound nucleus processes is seen in the fact that the cross sections for  $(\alpha, pxn)$  reactions are of the same order of magnitude as  $(\alpha, xn)$  cross sections. Their explanation rests strongly on the supposition that the ejection of high energy protons, deuterons, and tritons occurs leading to residual intermediate nuclei of low excitation energy, which then escape from fission. This unique description of the escape of charged particle emission reactions from fission competition is believed to have wide application for the explanation of spallation cross section data in the heaviest element region.

Fission yield curves for  $\text{Pu}^{238}$  and  $\text{Pu}^{239}$  have been constructed from the production cross sections (mass chain yield plus direct production) for the isotopes  $\text{Br}^{82,83}$ ,  $\text{Sr}^{89,91,92}$ ,  $\text{Ru}^{105}$ ,  $\text{Cd}^{115,115m,117}$ ,  $\text{I}^{131,133}$ ,  $\text{Ba}^{139,140}$ ,  $\text{Ce}^{143,145}$ ,  $\text{Nd}^{147}$ ,  $\text{Eu}^{156,157}$ ,  $\text{Tb}^{161}$ . The more complete curves for  $\text{Pu}^{239}$  show a change with increasing energy from asymmetric to symmetric fission for about 40 Mev helium ions accompanied by an increase in number of neutrons lost, as determined by the best fit of reflection points. Integration of the fission yield curves gives total fission cross sections for various energies which, when combined with the appropriate total spallation cross sections, define a total reaction cross section function consistent with a nuclear radius parameter in the range of  $1.3 - 1.6 \times 10^{-13}$  cm.

Further investigations in the present series should elucidate the effects of Z and A upon fission competition.



SPALLATION-FISSION COMPETITION IN HEAVIEST ELEMENTS;  
HELIUM ION INDUCED REACTIONS IN PLUTONIUM ISOTOPES

Richard A. Glass, Robert J. Carr,  
James W. Cobble, and Glenn T. Seaborg

Radiation Laboratory  
and Department of Chemistry and Chemical Engineering  
University of California, Berkeley, California

June 1956

A great deal of work has been done on the distribution in the yields of the products produced from the fission of nuclides over the entire range of atomic numbers. Further, these investigations included many kinds of incident projectiles covering a wide range of energies.<sup>1</sup> A considerable amount of work has also been done on the excitation functions for spallation reactions of various kinds throughout the periodic system over a wide range of energies.<sup>2</sup> Whenever proper energetic and other conditions for both are met, competition between the two types of reactions occurs and the results of the investigations of such competitive reactions are often very interesting.<sup>3-8</sup>

The present paper is the first in a series from this laboratory in which somewhat detailed investigations of the competition between spallation and fission reactions in the heaviest nuclides ( $Z \geq 88$ ) will be described. The program emphasizes the region where the compound nucleus model of the nucleus usually has been applied ( $<50$  Mev) and involves preponderantly bombardments with charged particles (protons, deuterons, helium ions and heavier ions). Although fission can be induced at even lower atomic numbers<sup>9-13</sup> such as lead ( $Z = 82$ ) and bismuth ( $Z = 83$ ) at these comparatively low excitation energies, the competition in this region is still highly in favor of spallation reactions.<sup>14,15</sup>

As the nuclear charge is increased, fission becomes the predominant reaction at about thorium<sup>6,16</sup> ( $Z = 90$ ), and the incomplete data which have been available until recently indicate that the spallation yields continue to change above thorium. It thus appears that a change in the atomic number of the compound nucleus of even a few units can greatly influence the relative spallation and fission yields in this critical region. The

question as to how small the spallation yield becomes at the highest atomic numbers is of special interest. The successful production of the new element mendelevium by the reaction  $^{17}\text{E}^{253}(\alpha, n)\text{Mv}^{256}$  involved a product-nucleus of atomic number 101, so it is evident that the spallation yields are not completely suppressed for these highest charge nuclides.

That the data on the heaviest elements will require a more complex explanation than a simple atomic number dependence of fissionability follows from the observation that fission competition does not affect the various spallation reaction yields from a given target nuclide to the same extent. The spallation yields differ in such a way as to suggest, among other things, that products apparently formed from direct or partial interaction, in which compound nucleus formation is avoided, are relatively favored. In addition, from one target nuclide to another in the uranium-plutonium region over a range of atomic numbers, a common spallation reaction pattern prevails; this is characterized by successively decreasing maximum cross sections for (p or d or  $\alpha$ ,xn) reactions for x greater than two, significant high energy extensions ("tails") for all excitation functions, and charged particle emission cross sections of equal prominence with neutron emission cross sections. This is quite different from the pattern for the lead-bismuth region which is dominated by systematic (p or d or  $\alpha$ ,xn) excitation functions of roughly comparable shape and magnitude.<sup>14,15</sup>

The number of excitation functions of the type (p,xn), (p,pxn), (p,2pxn), (d,xn), (d,pxn), (d,2pxn), ( $\alpha$ ,xn), ( $\alpha$ ,pxn), ( $\alpha$ ,2pxn), etc. which can be ultimately measured is influenced or determined by the availability of target nuclide material, and, in so far as detection based upon radioactivity is used, by the half-lives of the products. Investigations already in progress in this laboratory involve such target nuclides as Th<sup>232</sup>, Pa<sup>231</sup>, U<sup>233</sup>, U<sup>235</sup>, U<sup>238</sup>, Np<sup>237</sup>, Pu<sup>238</sup>, Pu<sup>239</sup>, Pu<sup>240</sup>, Pu<sup>242</sup>, Am<sup>241</sup>, Am<sup>243</sup>, Cm<sup>242</sup>, Cm<sup>244</sup>, Bk<sup>249</sup>, Cf<sup>249</sup>, Cf<sup>252</sup>, and E<sup>253</sup>.

For a number of cases the program also includes the investigation of the distribution in fission product yields for a number of energies in this region: 20-50 Mev helium ions, 10-25 Mev deuterons and 10-30 Mev protons. As the energy at which fission is induced is increased the contribution of symmetric fission is demonstrated through the appearance of a more shallow dip between the two peaks in the fission yield distribution curve. This peak-to-trough ratio decreases as the energy is increased until a sym-

metrical, single peaked curve is obtained, and it is hoped that the data will establish how these phenomena vary with atomic number, nuclear type, and incident projectile.

It is believed that this broad investigation of the competition between spallation and fission in the region of the heaviest elements can also furnish data which will be useful in further elucidating the mechanism of the fission process. It is likely that the results will ultimately indicate the overall pattern for the effect of changing nuclear charge and mass upon the ratios of the various spallation to fission yields as well as upon the magnitude and shape of the various spallation excitation functions, and the results should provide other information such as the possible influence of odd-even effects in the target and intermediate compound nuclei. Any correlation with the rapidly accumulating information on spontaneous fission and resonance effects in neutron induced fission would be of special interest.

The present paper will be concerned specifically with the various helium ion induced reactions in  $\text{Pu}^{238}$  and  $\text{Pu}^{239}$ . In addition, less complete data have been obtained for  $\text{Pu}^{242}$  to allow a further comparison of the effect of changing the mass of the compound nucleus upon the yields of certain specific spallation products. Unique features of these types of reactions will be discussed including possible mechanisms for the nuclear processes involved.

## II. EXPERIMENTAL PROCEDURES

### A. General

Bombardments with helium ions of energy up to about 50 Mev and deuterons up to about 25 Mev energy are performed on the 60-inch cyclotron of the Crocker Laboratory. Bombardments with protons of up to about 30 Mev energy are to be accomplished with the linear accelerator of the Radiation Laboratory. The well collimated external cyclotron beam of up to 20 microamperes particle current is degraded by weighed aluminum foils to the desired energy.<sup>18</sup> The target isotope material is usually deposited on a 10 mil aluminum backing foil shaped in the form of a small "hat". This "hat" and the energy degrading foils along with a 1 mil cover foil

(which serves to protect the target material and also to trap any recoiling fission products) are mounted in a water-cooled Faraday cup type of combined holder and ion chamber. The beam currents so produced are fed into a standard type current integrator, and are also recorded continuously. The technique just described, adapted to bombardments in which the entire target is to be dissolved and analyzed for products, is sometimes varied by analyzing only a "catcher" foil which has been placed next to the target to retain forward recoiling spallation product nuclei.<sup>17</sup>

The target isotope, in nearly all cases essentially free from other isotopes of the element, is ordinarily electroplated as the hydrated oxide on to the aluminum or other metallic backing "hat". Approximately 0.1-1 mg can be plated over the 1.2 cm<sup>2</sup> area. Pains are taken to insure that the target material is uniform as required for absolute cross section measurements. To this end activity profiles for the highly alpha radioactive targets are determined through a movable pinhole collimator and occasionally radioautographs are taken for representative targets. The amount of target material plated is determined by assaying each target plate in the appropriate standard alpha counter or calibrated low geometry counter followed by calculating the atom density from the specific activity. Assaying of the dissolved target solution after bombardment usually provides a method of checking this amount. Additional checks are made in some cases by weighing the "hat" before and after the plating (for Th<sup>232</sup>, U<sup>235</sup>, and U<sup>238</sup>). Thin metal foil targets (available for Th<sup>232</sup>, U<sup>235</sup>, and U<sup>238</sup>) and targets made by slurring the material on to the "hat" in aqueous suspension and drying are sometimes used.

After each bombardment, a suitable time is allowed for decay to reduce the frequently intense short-lived beta and gamma radioactivities in the target and also to allow short-lived fission product chain products to decay to their longer-lived daughters. The usual procedure of taking one long-lived member of a given mass decay chain to obtain the yield of that mass chain is used and consequently it is convenient to let some of the short-lived parent activities decay before chemical separation. The target material, target backing plate, and aluminum cover foil are all dissolved in acidic solutions containing known amounts of fission product "carriers" (5 - 20 mg for each element to be removed). The solution also contains

aliquots of standardized actinide element "tracer" solutions by which the chemical yields of the spallation products can also be determined. The tracers used are alpha particle emitting isotopes, e.g., Pa<sup>231</sup>, U<sup>233</sup>, Np<sup>237</sup>, Pu<sup>239</sup>, Am<sup>243</sup>, and Cm<sup>244</sup>, whose long half-lives preclude their being formed in important amounts in ordinary 1 - 15 microampere-hour bombardments.

The fission product activities and their inactive carriers, as well as the spallation product activities and their tracers, are isolated in a series of chemical separations, including precipitations, extractions, and ion exchange column elutions. Operations are performed first on the entire target solution (except for foil targets when aliquots are used) to separate groups of elements and later on these groups to finally isolate the isotopes of the desired individual elements.

After purification the fission product activities with carriers are mounted on tared aluminum "hats", weighed to determine chemical yield, and counted repeatedly either by automatic sample counters or individually at proper times to allow necessary resolution of the usually several components present in the decay curves for each element. The beta counters are of the argon and chlorine-filled geiger tube type (end window, Amperex 100C tube).

Suitable corrections must be applied for backscattering, self-scattering and self absorption, air and window absorption, geometry, coincidence losses, and branching in the decay schemes. For the scattering and absorption, use is made of the corrections determined under similar conditions by others.<sup>19-22</sup> All resolved decay data are corrected to the end of bombardment and suitable corrections are made for those isotopes whose half-lives are so short that they decay appreciably during the 2-4 hr bombardments. Accidental changes of the cyclotron beam intensity or short-time interruptions of the cyclotron occasionally require further decay corrections. Errors involved in determining the absolute fission yield of any isotope are about  $\pm 25$  percent, although the error in total mass yield may be greater due to independent yields of isobars of higher atomic number than the isobar assumed to adequately represent the entire mass chain yield. Preliminary results of independent yields indicate that this effect may amount in some cases to greater than 50 percent.<sup>23</sup> Fission product isotopes isolated from one or more target materials include Br<sup>82,83</sup>, Sr<sup>89,91,92</sup>, Y<sup>90,91,93</sup>, Zr<sup>95,97</sup>, Nb<sup>95,96</sup>, Mo<sup>99</sup>, Ru<sup>103,105,106</sup>, Pd<sup>109,112</sup>, Ag<sup>112,113</sup>,

Cd<sup>115m,115,117</sup>, Te<sup>129m,132</sup>, I<sup>131,133</sup>, Ba<sup>139,140</sup>, La<sup>140</sup>, Ce<sup>141,143,144,145</sup>, Pr<sup>142,143</sup>, Nb<sup>147</sup>, Eu<sup>156,157</sup>, Gd<sup>159</sup>, Tb<sup>161</sup>.

The carrier free spallation products are deposited on platinum plates either by evaporation from aqueous solution, electroplating, or volatilization from a tantalum filament in vacuum at about 1800°C. Total alpha counting rates are determined in a 52 percent geometry argon flow ionization chamber. Resolution of the gross alpha activity into the various separate alpha activities present is made by standard alpha pulse analysis.<sup>24</sup>

Radiations from isotopes undergoing electron capture decay (electrons and x-rays) are measured with a windowless beta proportional counter. Electron capture counting efficiencies are being determined for some of the nuclides<sup>25</sup> involved and approximate values for other species are estimated.

The thin target formula for the case of a non-uniform beam collimated to strike within a uniform target area applies for the cross section calculations. An approximate assignment of errors for the factors entering into the calculations is as follows: integrated beam intensity, ± 1 - 5%, due mainly to target alignment difficulty, electroplated target density, ± 10%, due to non-uniformity; disintegration rates for negatron emitting fission products, ± 20 - 25%, due mainly to counting correction uncertainties; disintegration rates for alpha particle emitting spallation products, ± 10%; disintegration rates for electron capture unstable products, ± 20 - 25%, due mainly to counting efficiency uncertainties. These errors can be combined to give the following average total errors: fission product cross sections, ± 25%; spallation cross sections for alpha radioactive products, ± 15%; spallation cross sections for electron capture radioactive products, ± 25%. The beam energy uncertainty is about ±0.8 Mev.

B. Present Plutonium Bombardments

The milligram quantities of plutonium isotopes available for the helium bombardments varied in isotopic purity from >99 percent for Pu<sup>239</sup> to 93.8 percent for Pu<sup>238</sup> (5.8 percent Pu<sup>239</sup> and small amounts of Pu<sup>240</sup>, Pu<sup>241</sup>, and Pu<sup>242</sup>) to 37.8 percent for Pu<sup>242</sup> (58.6 percent Pu<sup>238</sup>, 3.4 percent Pu<sup>239</sup>, and small amounts of Pu<sup>240</sup> and Pu<sup>241</sup>), necessitating the subtraction of spallation yield contributions from contaminating isotopes for the latter two isotopes. The Pu<sup>238</sup> target material was produced by

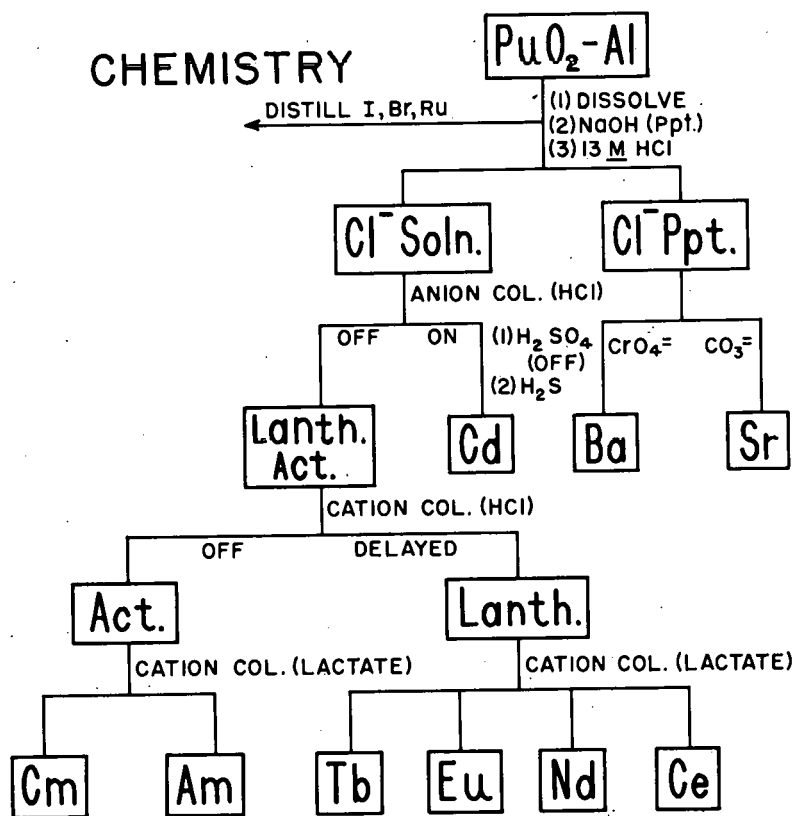
the intense neutron irradiation of  $\text{Np}^{237}$  to form  $\text{Np}^{238}$ , which subsequently decayed to  $\text{Pu}^{238}$ , in the Materials Testing Reactor at Arco, Idaho. The electroplating procedure for target preparation and chemical separation procedures employed are outlined in the appendix I and Fig. 1. The spallation product tracers,  $^{26}\text{Cm}^{244}$  and  $\text{Am}^{243}$ , were satisfactory for  $\text{Pu}^{238}$  and  $\text{Pu}^{239}$  bombardments but not for  $\text{Pu}^{242}$  since  $\text{Cm}^{244}$  is the  $(\alpha, 2n)$  reaction product. For this and other reasons the  $\text{Pu}^{242}$   $(\alpha, xn)$  cross sections were determined relative to the  $\text{Pu}^{238}$  and  $\text{Pu}^{239}$  cross sections (using targets prepared by the slurring method) which were in turn determined absolutely.

Important spallation products from  $\text{Pu}^{239}$  bombardments are illustrated for orientation purposes in an isotope diagram, Fig. 2, with squares enclosing those actually observed. Modes of formation and possible further reactions are indicated along with total energy requirements (thresholds) for particle emission reactions and also half-lives for all species.

Since the 60-inch cyclotron is also used to accelerate deuterons, the helium ion beam was occasionally monitored to detect possible deuteron contamination of the beam. Although range and cyclotron resonance data<sup>27</sup> clearly showed that any possible deuteron contamination should be unimportant, monitoring was considered worth while because even a several percent deuteron contamination could possibly lead to high apparent  $(\alpha, pxn)$  cross sections. The monitor reaction was the  $\text{Bi}^{209}(d, p)\text{Bi}^{210}$  reaction whose cross section<sup>14</sup> is known and which leads to beta activity;  $\text{Bi}^{209}(\alpha, xn)$  or  $\text{Bi}^{209}(\alpha, pxn)$  reactions all lead to alpha emitters at the energies tested (ca. 30 Mev). Deuteron contamination was found in this manner to be  $\leq 0.1$  percent.

### III. EXPERIMENTAL RESULTS

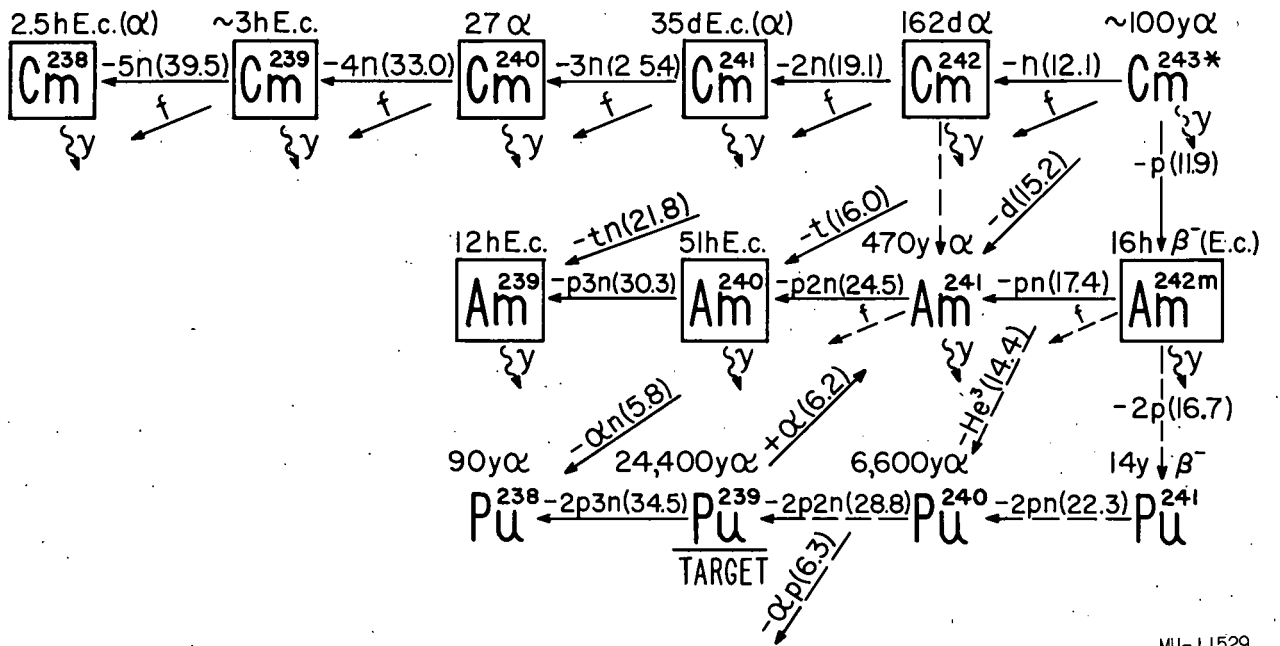
The individual cross sections obtained at each energy are listed for both spallation and fission products for the various plutonium isotopes in Tables 1 - 3. The spallation cross sections have been plotted as a function of energy in Figs. 3 - 5. The individual fission product cross sections, when plotted, yielded curves which are represented by Figs. 6 and 8. Integration of such curves then gave the total fission cross sections which are also included in the tables. Both the fission and spallation data



MU-11526

Fig. 1





MU-11529

Fig. 2

together with the percent of the total observed cross sections attributable to spallation are plotted in Figs. 7 and 9, which immediately demonstrate the relative proportion of the various types of reactions. The total observed cross sections themselves for  $\text{Pu}^{238}$  and  $\text{Pu}^{239}$  are compared with theoretical curves in Fig. 10. The counting procedures used are briefly described in Appendix I. Some of the yields were determined by counting the radiations from nuclides decaying by electron capture ( $\text{Am}^{239}$ ,  $\text{Am}^{240}$ ,  $\text{Cm}^{241}$ ): the counting efficiencies used in these cases are also described in Appendix I.

The spallation products themselves are graphically illustrated in a more conventional manner in Figs. 3 - 5. Unfortunately,  $\text{Am}^{241}$ , which may have been a significant spallation product nuclide from the  $(\alpha, pn)$  reaction on  $\text{Pu}^{239}$  could not be determined with any accuracy, because this isotope was present in the  $\text{Am}^{243}$  tracer solution that was added to the dissolved target. Further, the high specific activity of the plutonium targets precluded any determination of the  $(a, an)$  reaction yields for these isotopes, although, according to information gained from other target isotopes,<sup>28,29</sup> cross sections might be in the range above 10 mb at the highest energies. It was also impossible to determine the yield of the  $(a, \gamma)$  product from  $\text{Pu}^{239}$  since the  $\text{Cm}^{243}$  so formed has too long a half-life and, incidentally, also has the same alpha particle energy as  $\text{Cm}^{244}$  which was used for the chemical yield tracer. The yields of  $\text{Cm}^{242}$  and  $\text{Cm}^{246}$  formed from the  $\text{Pu}^{238}$  and  $\text{Pu}^{242}$   $(a, \gamma)$  reactions irrespectively, could not be determined for similar reasons. However, experience on  $(a, \gamma)$  reactions<sup>30</sup> leads one to expect very small cross sections for these processes. It must be noted that since the first americium-curium separation takes place some four hours after the end of the bombardments, some of the  $\text{Am}^{239}$  from the target  $\text{Pu}^{238}$  could be formed by  $\text{Cm}^{239}$  decay. Thus the excitation function for  $\text{Am}^{239}$  production Fig. 3 is labeled  $(\alpha, p2n) + (\alpha, 3n)$ , although the contribution from the  $(\alpha, 3n)$  reaction is undoubtedly the smaller. The yield of  $\text{Cm}^{238}$  from the  $\text{Pu}^{239}$   $(\alpha, 5n)$  and the  $\text{Pu}^{238}$   $(\alpha, 4n)$  reactions is determined only very approximately because it was determined by alpha particle counting using an alpha branching ratio (1.8 percent) estimated from alpha systematics. The yield of  $\text{Cm}^{239}$  from the  $\text{Pu}^{239}$   $(\alpha, 4n)$  reaction is also very approximate, due to the difficulties in the resolution of decay curves obtained from measurements with proportional counters. For  $\text{Pu}^{242}$ , the  $(\alpha, 2n)$  excitation function

Table I. Pu<sup>238</sup> spallation and fission cross sections.

Product	<u>Cross Section ( mb. )</u>						
	25.2 Mev	28.7	30.2	33.0	36.6	42.2	47.4
<u>Spallation</u>							
Cm <sup>241</sup> ( $\alpha, n$ )	4.6	7.1		6.0	3.1	2.5	2.8
Cm <sup>240</sup> ( $\alpha, 2n$ )	15	14	9.9	8.9	4.7	4.3	3.5
Cm <sup>238</sup> ( $\alpha, 4n$ )					0.002	0.19	0.26
Am <sup>240</sup> ( $\alpha, pn$ )		2.6	1.9	3.3	15	13	8.0
Am <sup>239</sup> ( $\alpha, p2n$ ) <sup>a</sup>		3.0	5.2	6.9	27	22	18
$\Sigma\sigma_s$	20	27	23	25	50	42	33
<u>Fission</u>							
Sr <sup>91</sup>		14		17	12	11	29
Cd <sup>115</sup> +Cd <sup>115m</sup>	10	23	28	43	38	43	57
Ba <sup>140</sup>	10	12	17	20	22	15	19
Ce <sup>143</sup>			25		34	22	
Nd <sup>147</sup>			17		23	20	
Eu <sup>156</sup>			2.8		3.6	3.7	
Tb <sup>161</sup>			0.48		1.9	1.0	
$\sigma_f$	430	640	980	1100	1000	1000	1400
$\sigma_f + \Sigma\sigma_s$	450	667	1000	1130	1050	1040	1430
% spall.	4.4	4.1	2.3	2.2	4.8	4.0	2.3

a. Product, and consequently cross sections, are for the sum of the ( $\alpha, p2n$ ) and ( $\alpha, 3n$ ) reactions.

Table II. Pu<sup>239</sup> spallation and fission cross sections.

Product	<u>Cross Section ( mb )</u>												
	20.2 Mev	24.0	24.5	26.8	27.5	34	38	39.2	40.7	43.8	44.3	46.0	47.5
<u>Spallation</u>													
Cm <sup>242</sup> ( $\alpha$ ,n)	1.1		0.84	1.1 <sup>a</sup>	1.3	2.4	2.2	1.8	0.97	1.5 <sup>a</sup>	1.6 <sup>a</sup>	2.6	0.82
Cm <sup>241</sup> ( $\alpha$ ,2n)			6.7	9.8	12	9.5	9.0	8.1	7.3	7.5	5.8	4.2	4.6
Cm <sup>240</sup> ( $\alpha$ ,3n)			10 <sup>-5</sup>	1.2	0.86	3.5	4.5	3.6	2.3	2.7	3.0	2.1	1.9
Cm <sup>239</sup> ( $\alpha$ ,4n)									0.8				0.6
Cm <sup>238</sup> ( $\alpha$ ,5n)												0.004	
Am <sup>242m</sup> ( $\alpha$ ,p)	0.030		0.58	0.72	0.29	1.3	0.96	0.58	1.1				0.56
Am <sup>240</sup> ( $\alpha$ ,p2n)				0.30		5.2	7.7	9.6	14	15		13	17
Am <sup>239</sup> ( $\alpha$ ,p3n)							<0.3	<0.4				$\leq 0.4$	$\leq 0.3$
$\Sigma\sigma_s^b$	1.1	(7.5)	8.1	13	15	22	25	24	26	28	27	23	26
<u>Fission</u>													
Br <sup>82</sup>			0.05 <sup>c</sup>										
Br <sup>83</sup>			0.23										
Sr <sup>89</sup>	0.06	0.95	2.0		3.4	4.3	15 <sup>d</sup>		9.5	16		14	15
Sr <sup>91</sup>	0.11	2.1	3.5			5.4	14 <sup>d</sup>		15	26		17	34
Sr <sup>92</sup>	0.13	1.4				6.2	13		13			17	21
Ru <sup>105</sup>						8.6							

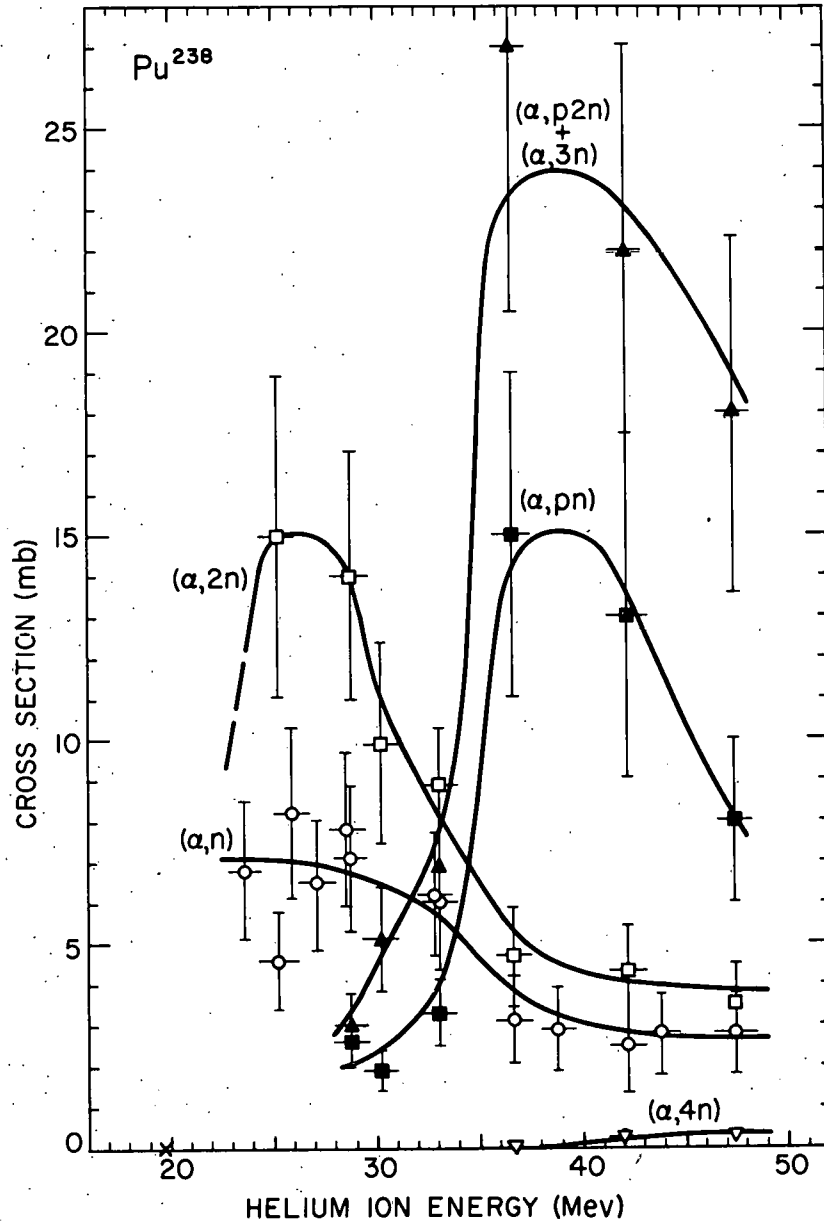
$\sigma_s^b$	1.1	(7.5)	8.1	13	15	22	25	24	26	28	27	23	26
<u>Fission (cont'd)</u>													
Cd <sup>115 +</sup> Cd <sup>115m</sup>	0.048	0.7 <sup>e</sup>	1.4		2.6	5.3	9		38	68		55	
Cd <sup>117</sup>	0.04					6.2	18		23			48	85
I <sup>131</sup>		1.6											
I <sup>133</sup>		2.1											
Ba <sup>139</sup>	0.29		5.4		5.7				16			20	21
Ba <sup>140</sup>	0.19	3.1	4.5		6.3	12 <sup>d</sup>	16 <sup>d</sup>		9.5	19		18	18
Ce <sup>143</sup>		3.0				11							
Ce <sup>145</sup>						14							
Nd <sup>147</sup>												12	
Eu <sup>156</sup>		0.32				0.7						2.9	
Eu <sup>157</sup>		0.30										2.3	
Tb <sup>161</sup>												1.9	
$\sigma_f$	5.0	66	125		160	310	510		780	1460		1260	1900
$\sigma_f + \sum \sigma_s$	6.1	74	133		175	332	535		806	1490		1280	1930
% spall.	18	10	6.1		8.6	6.6	4.7		3.2	1.9		1.8	1.3

- a. Value thus indicated has been adjusted to the  $(\alpha, n)$  excitation function and serves as a basis for estimating all other cross sections, otherwise only of relative significance, at this energy.
- b. Values include measured or estimated cross sections only for observed products.
- c. Product is a shielded nuclide.
- d. Value indicated is an average of two determinations.
- e. Value interpolated from graph of peak to valley ratio of yield curves vs. energy.

Table III.  $\text{Pu}^{242}$  and  $\text{Pu}^{238}$  spallation cross sections.

Product	Cross Section (mb)						
	23.6	25.9	27.1	28.5	32.8	28.8	43.5
$\text{Pu}^{242}$ <sup>a</sup>							
$\text{Cm}^{244}(\alpha, 2n)$ <sup>b</sup>	103	116	70	68	30	24	35
$\text{Cm}^{242}(\alpha, 4n)$				0	1.8	8.6	8.3
$\text{Pu}^{238}$							
$\text{Cm}^{241}(\alpha, n)$	6.8	8.2	6.5	7.8	6.2	2.9	2.8

- a. Absolute cross sections were determined by referring relative cross sections to  $\text{Pu}^{238}(\alpha, 2n) \text{Cm}^{240}$  reaction cross sections, since targets were 58.6%  $\text{Pu}^{238}$ .
- b. Product and consequently cross section are for the sum of the  $(\alpha, 2n)$  and  $(\alpha, pn)$  reaction. Cross sections also small contributions from the  $(\alpha, 3n)$  reactions at the higher energies.



MU-11143

Fig. 3



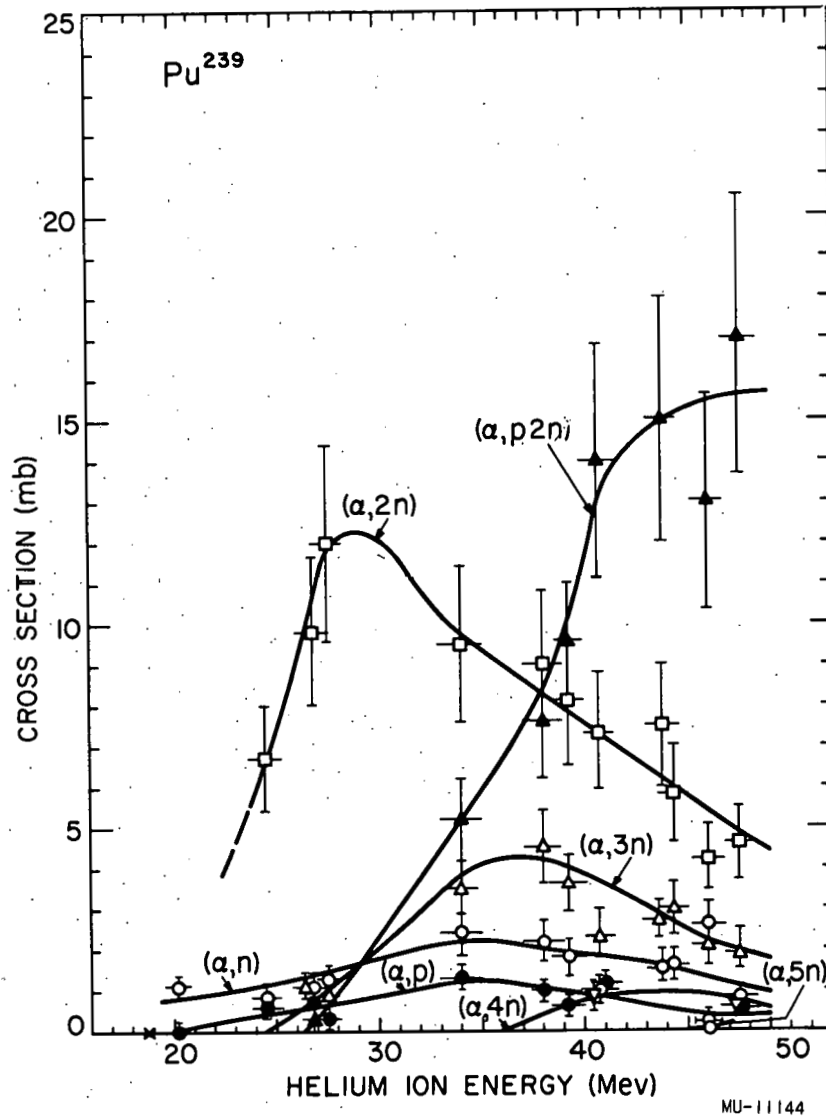


Fig. 4

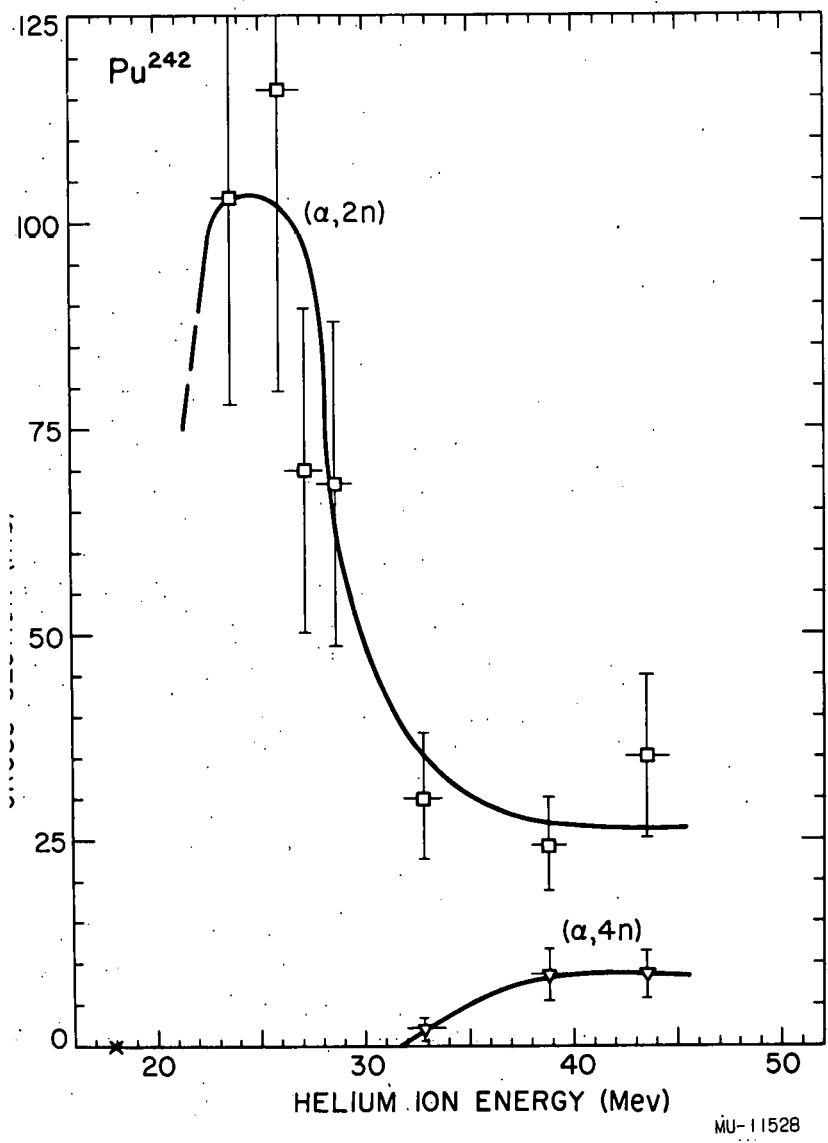
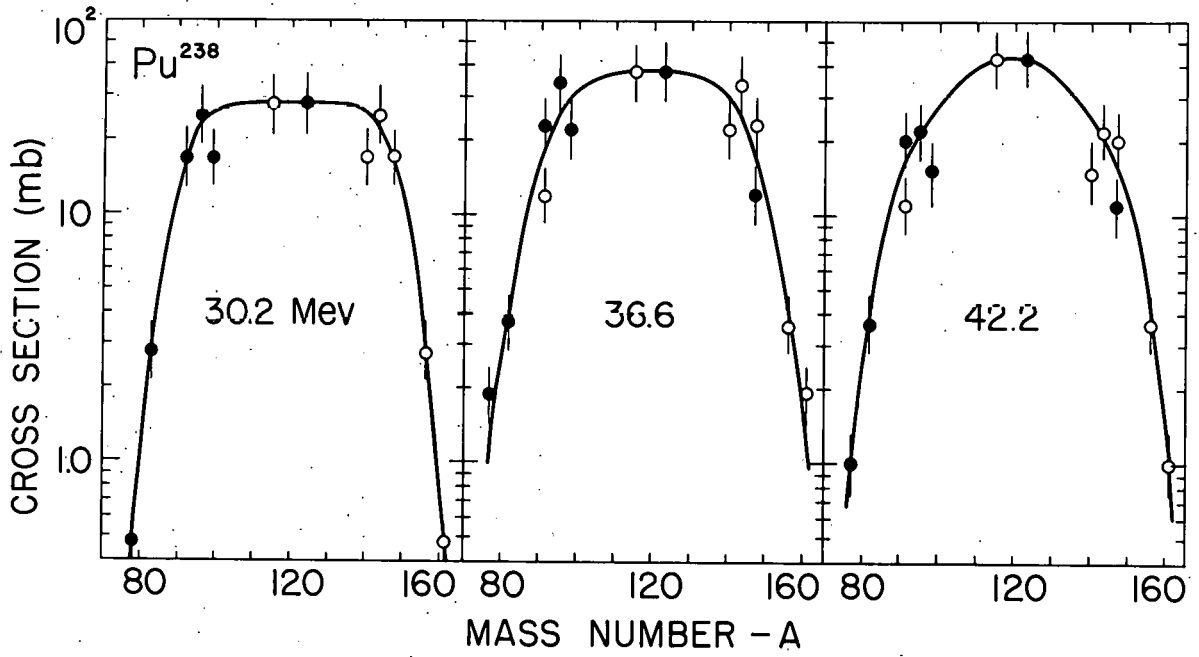


Fig. 5

MU-11528



MU-11504

Fig. 6

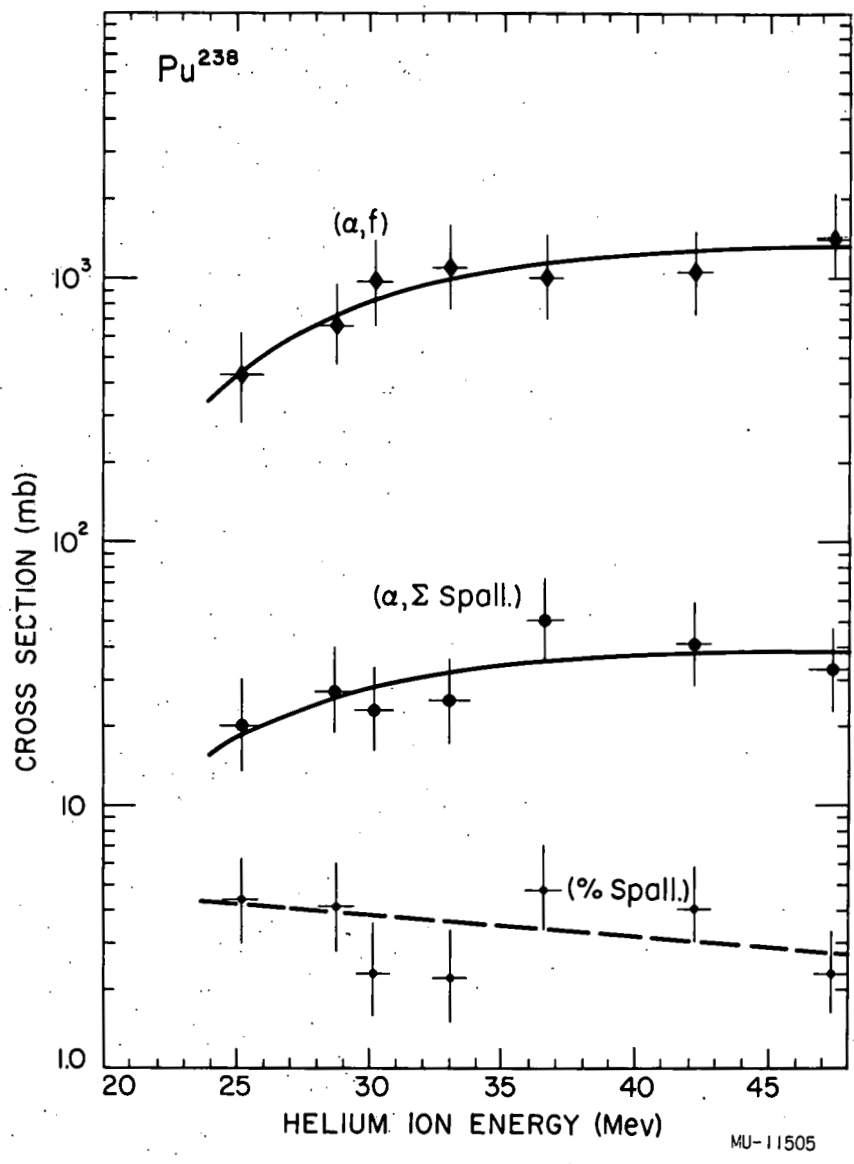


Fig. 7

MU-11505

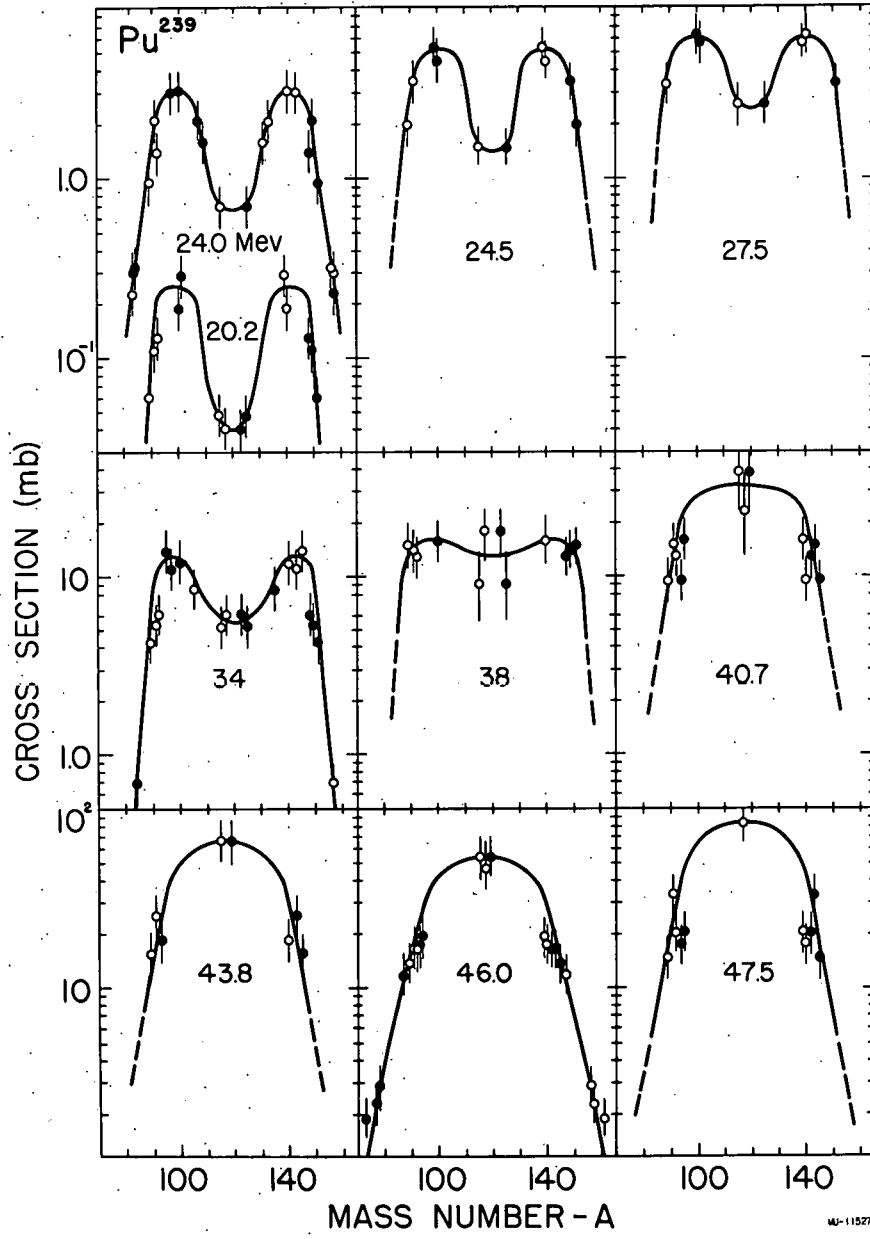


Fig. 8

W-1157

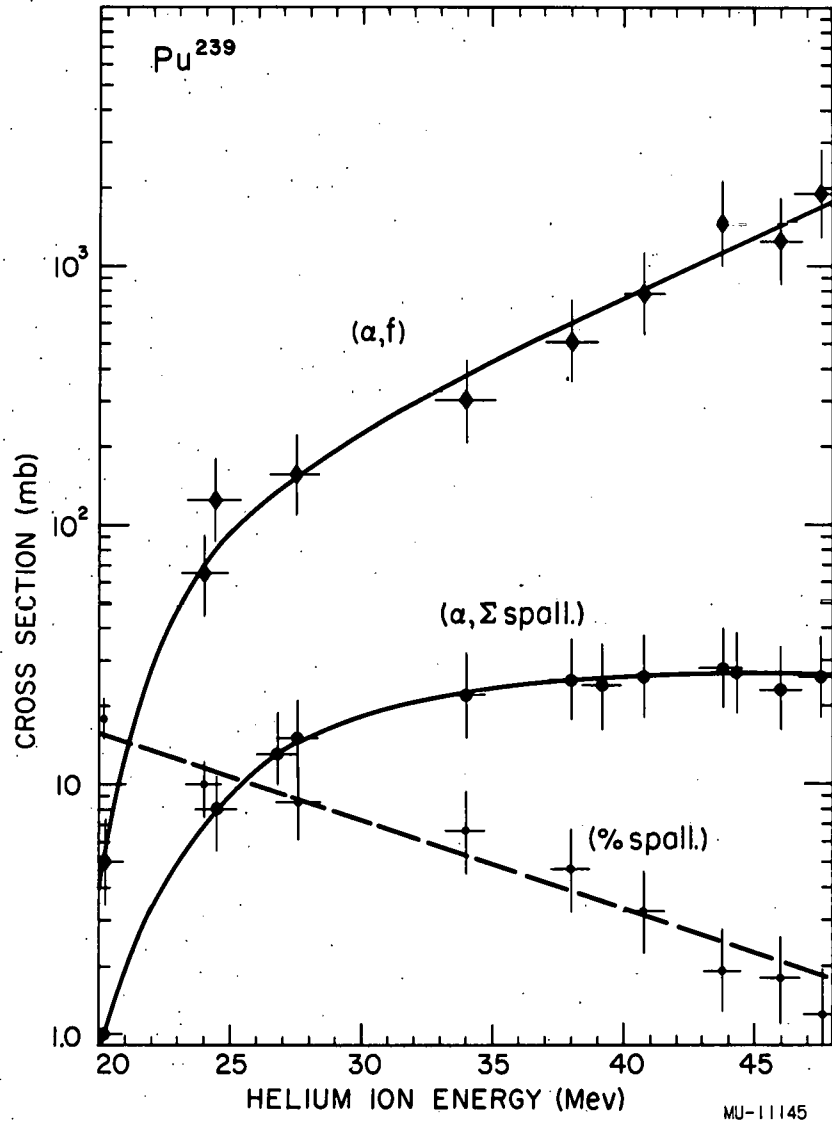


Fig. 9

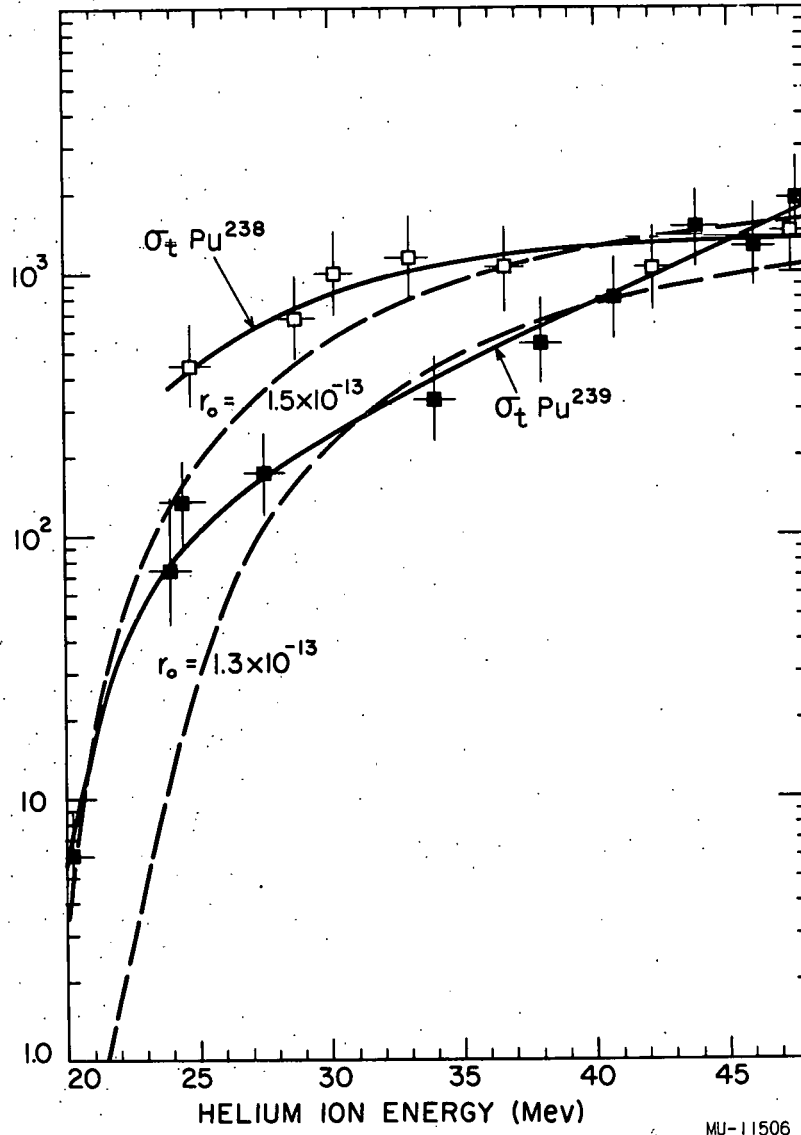


Fig. 10

27

contains some contributions from the  $(\alpha, 3n)$  reaction (since the alpha energies of  $\text{Cm}^{244}$  and  $\text{Cm}^{243}$  are indistinguishable to the pulse analyser) and the  $(\alpha, pn)$  reaction (since  $\text{Am}^{244}$  decays by beta decay to  $\text{Cm}^{244}$ ). The  $(\alpha, 4n)$  excitation function is also a composite for the  $(\alpha, 4n)$  and  $(\alpha, p3n)$  reactions for similar reasons.

Summation of all of the experimental fission and spallation cross sections for  $\text{Pu}^{238}$  and  $\text{Pu}^{239}$  leads to the results given in Fig. 10. Theoretical total cross section plots calculated from the statistical model<sup>31</sup> are shown for chosen values of 1.3 and 1.5 for the nuclear radius parameter,  $r_0$ . The agreement between the theoretical and experimental curves perhaps indicates that most major fission and spallation reaction products have been determined.

#### IV. DISCUSSION

It is clear from Fig. 7 and 9 that fission is the predominant reaction induced in plutonium by helium ions in the 20 - 50 Mev energy range as might be expected. The proportion that goes into fission generally exceeds 90 percent, a substantial increase over the fraction of reactions that go into fission when thorium is bombarded with particles in the medium energy range.<sup>6</sup> This competition with fission thus lowers the magnitude of the total cross section for spallation reactions. A careful consideration of the shapes and relative magnitudes of the spallation excitation functions shows a number of features not found with nuclides where competition with fission is not important. Only a part of this information on spallation reactions, principally the excitation function peaks for the  $(\alpha, 2n)$ ,  $(\alpha, 3n)$ , and  $(\alpha, 4n)$  reactions (see Figs. 3, 4, and 5), fits nicely into a general picture of compound nucleus formation followed by particle evaporation, and significantly it is the probabilities for these reactions that are greatly reduced by fission competition. The prominent  $(\alpha, pxn)$  reactions and high energy extensions ("tails") on the excitation functions likely result from interactions in which thermal equilibrium of a compound nucleus is not involved, such as direct interaction of the "knock-on" type. However, detailed mechanisms of the processes occurring cannot presently be given.



28

Let us consider for illustrative purposes the case of the helium ion induced spallation reactions in  $\text{Pu}^{239}$  (Fig. 4), for which the most data have been obtained. For purposes of illustration the parent compound nucleus,  $\text{Cm}^{243}$ , and the various possible follow-up reactions with their energetic thresholds (with no allowance for potential barriers) have been indicated in Figure 2. This nucleus can undergo particle evaporation (neutron, proton, or heavier particle), fission, or de-excitation by gamma ray emission (although this is very improbable for the compound nucleus.<sup>32</sup> The same is true for each of the other intermediate compound nuclei, and it is evident that the situation differs from the usual cases hithertofore studied because of the fission competition which is present at each step. It is recognized that the compound nucleus may be by-passed, particularly for the  $(\alpha, n)$  and  $(\alpha, pxn)$  reactions, although even in these cases the residual nucleus may be left in an excited state subject to removal by the fission reaction in competition with particle or gamma ray emission.

The relative probability for fission compared to further spallation is a function of the excitation energy and particular nuclear character of each intermediate compound nucleus. Not much is presently known, however, about how this relative probability varies with either of these factors. Important in this respect will be how the probability for fission of the intermediate compound nuclei varies with atomic number ( $Z$ ), mass number ( $A$ ), and with odd and even numbers of neutrons and protons. The parameter<sup>33</sup>  $Z^2/A$  is of importance in determining the probability for low energy fission<sup>34,35</sup> and spontaneous fission<sup>36,37</sup>. Although the same parameter may not apply to fission in the energy range under discussion here any applicable general dependence on  $Z$  and  $A$  is certainly of interest.

With this brief outline let us proceed to examine the individual reactions: first the  $(\alpha, xn)$  excitation functions for both compound and non-compound nucleus contributions, then the important  $(\alpha, pxn)$  reactions, and finally the fission cross sections themselves.

As stated above, in a qualitative way the generally low values for the cross sections in the spallation excitation functions are readily understood to indicate that fission is claiming most of the compound and intermediate nuclei. The cross section for the  $\text{Pu}^{239} (\alpha, 2n)$  reaction is in the range of 10 millibarns in contrast to the  $(\alpha, 2n)$  cross sections of about

1,000 millibarns at similar energies for lead<sup>15</sup> and bismuth<sup>14</sup> where competition with the fission reaction is not a factor.

More quantitatively the success with which fission competes with neutron emission is revealed in the relative  $(\alpha, xn)$  excitation functions (Figs. 3, 4, and 5), which record in each cross section value the combined survival from fission of one or more intermediate nuclei along a neutron emission path. The effect is illustrated by the  $(\alpha, 2n)$ ,  $(\alpha, 3n)$ , and  $(\alpha, 4n)$  excitation functions for Pu<sup>239</sup> (Fig. 4), which exhibit decreasing maximum cross section values in the ratio 1:0.3:0.07. In contrast the cross sections at the peaks of the excitation functions for the identical reactions among lead<sup>15</sup> and bismuth<sup>14</sup> isotopes actually increase in the approximate ratio 1:1.4:1.4. For an interpretation of such a decrease in peak heights among fissionable elements Meinke, Wick, and Seaborg<sup>5</sup> previously suggested as part of an explanation for the results obtained by them in a study of spallation-fission competition in the thorium-uranium region that the probability for fission, or  $\Gamma_f$ , increases with energy at about the same rate as the probability for neutron emission, or  $\Gamma_n$ , for nuclei excited to a similar energy range to that under investigation here.

Consideration of the plutonium  $(\alpha, xn)$  excitation functions from a compound nucleus viewpoint, including a calculation of rough  $\Gamma_f / \Gamma_n$  values (outlined in appendix II) leads to the same conclusion that  $\Gamma_f / \Gamma_n$  is not a strong function of energy in the energy range under investigation (ranging in value between 1 and 7 for the curium isotopes in the helium ion bombardment target nuclei Pu<sup>238</sup>, Pu<sup>239</sup>, and Pu<sup>242</sup>). The analysis, consisting of calculations of mean neutron emission branching ratios and then  $\Gamma_f / \Gamma_n$  values for intermediate nuclei from the  $(\alpha, xn)$  excitation function peaks (omitting the  $(\alpha, n)$  reaction), has been extended to all available excitation function data for the elements thorium and above. The results show that among the isotopes of an element there is a gradual decrease in  $\Gamma_f / \Gamma_n$  with increasing mass number but no significant variation among isotopes of several elements lying approximately the same distance from the line of beta stability, except that in the thorium region  $\Gamma_f / \Gamma_n$  decreases noticeably. Thus the empirical observation from the bombardment program in progress that the  $(\alpha, xn)$  excitation functions are similar for corresponding reactions among isotopes (of elements uranium and above) in the same region of the Heisenberg valley is interpreted to mean

that the ratios of the level width for fission to the level width for neutron emission are likewise similar. The inescapable conclusion from these data is that an atomic number effect is not dictating a continuous decrease in spallation cross sections due to a general increased fissionability of nuclides with increasing  $Z$  and also that  $Z^2/A$  is not a promising parameter for interpretation of fission with medium excitation energies.

The effect of  $A$  on the relative probability for fission competition among the plutonium isotopes is striking. It is possible to compare the yields of identical reactions on target nuclei of the same type (i.e. both even-even) in the case of the  $\text{Pu}^{238}(\alpha, 2n)$  and  $\text{Pu}^{242}(\alpha, 2n)$  reactions (Figs. 3 and 5). The yield from  $\text{Pu}^{242}$  is about seven times greater than that from  $\text{Pu}^{238}$  throughout the energy range. Thus in this region and range of  $A$  there is a clear effect; i.e. the relative probability for fission increases as  $A$  decreases. It may be noted that the yield of the  $\text{Pu}^{242}(\alpha, 4n)$  reaction (Fig. 5) is also greater than that of the  $\text{Pu}^{238}(\alpha, 4n)$  reaction (Fig. 3), showing the same effect for change in  $A$ . Both of these observations demonstrate that  $\Gamma_f/\Gamma_n$  increases as  $A$  decreases.

The continuing yields at the highest energies for the  $(\alpha, n)$  reaction (Figs. 2 and 3) indicate some failure of the compound nucleus picture, with direct interactions between the constituents of the projectile and those of the struck nucleus apparently important. Such direct interactions are certainly also involved in the explanation of the long tails seen in many of the other excitation functions (e.g. the  $(\alpha, 2n)$  excitation functions in Figs. 3, 4, and 5). Direct interaction interpretations for low energy reactions are not new<sup>38</sup> and are equally applicable to tails observed among excitation functions for lighter elements.<sup>15,39</sup> Among the heaviest elements non-compound nucleus mechanisms also play a role in aiding fission survival, which as we shall see is important for the  $(\alpha, pxn)$  reactions. The direct interaction mechanism implies that the  $(\alpha, n)$  product must be formed in large part by reactions in which the incident helium ion does not amalgamate with the struck nucleus. For this reaction the highly fissionable compound and intermediate nuclei can be completely avoided if the emitted neutron carries off sufficient energy to leave the residual nucleus with excitation energy below the fission threshold. In the case of reactions contributing to the "tails" of the excitation function for the  $(\alpha, 2n)$  and

$(\alpha, 3n)$  reactions, excited intermediate nuclei susceptible to fission exist prior to evaporation of the second and third neutrons after the initial knock-on reaction.

The  $(\alpha, xn)$  excitation functions, then, contain contributions from compound nucleus and knock-on mechanisms and should strictly be separated into these components for analysis. Since this division would be somewhat arbitrary it has been avoided and the aforementioned analysis for  $\Gamma_f / \Gamma_n$  values was performed with the total excitation function. A measure of the energy distribution of the emitted neutrons and protons would be very interesting from this point of view.

An important feature peculiar to this region is the comparable yields of the  $(\alpha, xn)$  and  $(\alpha, pxn)$  reactions (Figs. 3 and 4). The coulomb barrier to the outgoing proton makes the cross sections for the latter much lower than those for the former reactions in regions of high atomic number, for example, around lead,<sup>15,40,41</sup> where competition with fission is not a factor. These  $(\alpha, pxn)$  reactions in  $\text{Pu}^{238}$  and  $\text{Pu}^{239}$  are of the same order of magnitude as those around lead, while the  $(\alpha, xn)$  reactions have been greatly reduced.

Let us consider for the sake of completeness, whether the high  $(\alpha, pxn)$  compared to  $(\alpha, xn)$  yields in plutonium could be due to smaller competition with fission due to the lower  $Z$  for the intermediate compound nuclei possibly involved in the  $(\alpha, pxn)$  reactions, in which the proton would probably generally be the first particle evolved. Such an effect of  $Z$ , i.e. rather rapidly increasing fissionability with increasing  $Z$  for nuclei excited to these energies, has been tested by measuring the yields of the same spallation reactions over a wide range of  $Z$  for the target nuclei. Data already available from the general program of investigation of spallation-fission competition in this laboratory indicate that the ratio for spallation to fission yield does not steadily decrease with increasing  $Z$  for many such spallation reactions. For example, the cross sections for the  $(\alpha, 2n)$  reaction, which are of the order of ten millibarns for  $\text{Pu}^{238}$  and  $\text{Pu}^{239}$  (Figs. 2 and 3), also have about the same value for the lower  $Z$  target nuclide  $\text{U}^{233}$  and the higher  $Z$  target nuclides  $\text{Cm}^{244}$  (43) and  $\text{Cf}^{249}$  (44). There are indications that the yields for a number of other spallation reactions also have a surprisingly small variation with  $Z$ . Thus we are forced to conclude

that the increase of fissionability with the increase in  $Z$  is much too small to account in general for the low ratio of  $(\alpha, xn)$  to  $(\alpha, pxn)$  yields.

Since  $\Gamma_f / \Gamma_n$  is nearly constant with increasing energy of excitation (as concluded from the yields for  $(\alpha, xn)$  reactions in Appendix II) we can account for the relatively high yields of the  $(\alpha, pxn)$  reactions if we assume that the corresponding intermediate nuclei are formed in large part by a mechanism in which proton emission from a compound nucleus is not involved and are formed in a relatively low degree of excitation. Apparently these products are formed in large part by reactions in which the incident helium ion does not amalgamate with the struck target nucleus and the emitted nucleons (or combination of nucleons) come off with high energy leaving the nucleus in a state of small excitation. On this picture the high yield of the  $(\alpha, p2n)$  reaction might suggest that the outgoing particle is often a relatively high energy tritium nucleus rather than a proton and two neutrons; thus competition with fission is small because the intermediate nuclei involved do not go through a degree of high excitation. Preliminary experiments in this laboratory,<sup>45</sup> in which the actual yield of tritium produced in the helium ion bombardment of uranium was measured, show that a rather large yield of tritium is obtained. Thus emission of high energy protons, deuterons, and tritons could explain the relatively high yields of the  $(\alpha, pxn)$  reactions. The low yield of the  $(\alpha, p3n)$  reaction, Table IV, is in agreement with this picture for this reaction allows no apparent mechanism for the formation of intermediate nuclei which are all at low excitation energy and hence the yield is drastically reduced through the competition by the fission reaction. The fact that an  $(\alpha, pn)$  reaction peak was not observed<sup>46</sup> for  $\text{Pu}^{242}$  may be further evidence that compound nuclei are not involved for this reaction, since the effect of mass number which acts to increase the  $(\alpha, 2n)$  cross section for  $\text{Pu}^{242}$  compared to  $\text{Pu}^{238}$  target nuclei does not act proportionately to increase the yield of the  $(\alpha, pn)$  reaction. Another example of direct interaction is apparently the large yield of the  $(\alpha, \alpha n)$  reaction<sup>29</sup> in  $\text{U}^{238}$ .

Thus the conclusion seems inescapable, on the basis of several types of evidence, that direct interaction between the constituents of the projectile and those of the struck nucleus, i.e., processes other than compound nucleus formation, are taking place in a rather prominent manner. Effects

of this magnitude at the moderate energies involved (mainly some 20-40 Mev) were at first rather surprising. However, this heavy region is well suited to the study of such reactions because the slightly excited non-compound nuclei are favored over the more highly excited bona fide compound nuclei due to greater loss of the latter by competition with fission. The relative importance of stripping, knock-on, and pick-up reactions, or possible combinations of these, is not established on the basis of the present work. It seems likely that such mechanisms will also be important in this region of atomic number for reactions induced with heavy ions,<sup>47,48</sup> leading to the formation of nuclides of much higher atomic number than the target in such low degree of excitation that a measurable proportion of them can survive the competition with the fission reaction.

It would be interesting to see whether any effect due to nuclear type (i.e. even-even, even-odd, etc.) can be discerned and interpreted and the yields of the  $(\alpha,2n)$  reactions on the neighboring nuclides  $\text{Pu}^{238}$  and  $\text{Pu}^{239}$  can be studied from this point of view (Fig. 4). We find here similar excitation functions of approximately equal magnitudes with the peak at several Mev higher energy in the case of  $\text{Pu}^{239}$ . In a similar comparison of the excitation functions for the  $(\alpha,n)$  reaction on  $\text{Pu}^{238}$  and  $\text{Pu}^{239}$  (Figs. 3 and 4) the former shows the higher yield but its shape is not well enough defined to make a comparison of shapes meaningful. Thus  $\text{Pu}^{239}$ , in spite of a larger value for A, shows an equal and a smaller yield for these particular reactions ( $\alpha,2n$  and  $\alpha,n$  respectively) compared to  $\text{Pu}^{238}$ . However, a consideration of the nuclear types of the target, compound and product nuclei involved doesn't lead to any clear cut conclusion. Any elucidation of the effect of nuclear type apparently awaits more data of a type which might be forthcoming from following investigations in this program.

The distributions in the yields of the fission products were determined primarily for the purpose of estimating the fission cross sections at the various energies and therefore these rather laborious investigations were not sufficiently extensive nor accurate to draw many other conclusions concerning the details of the fission process itself. The yield of a fission product near the end of a given beta particle decay chain has been assumed to represent the entire yield for that mass number. As mentioned above this procedure can lead to errors greater than 50 percent in some individual cases<sup>23</sup>, especially for the heavy fission products, and hence the fission

cross sections are probably best considered to be lower limits. The commonly used procedure of reflecting the low and high mass peaks of the yield curves was utilized in order to complete the total fission product yield curves, which may introduce some additional error into the integration process for estimating the fission cross sections.

The total interaction cross sections, obtained as the sum of the fission and spallation cross sections (Fig. 9) lead to a reasonable value for the nuclear radius parameter<sup>31</sup> for both Pu<sup>238</sup> and Pu<sup>239</sup>, i.e.  $R^0$  equal about  $1.3-1.6 \times 10^{-13}$  cm. Another deduction, which can be made from the center of symmetry of the fission yield distribution curve, is the average number of neutrons emitted in connection with the fission process. Such considerations indicate, more clearly for Pu<sup>239</sup>, the emission of several more neutrons at the highest energies than at the lowest energies (Fig. 8). It seems likely that this increase in neutron emission comes largely from the fission fragments since, although pre-fission evaporation of up to 5 neutrons is energetically possible, fission competition interrupts most chains of neutron emission after the first few steps as was deduced from the sharply decreasing maximum cross section values for the Pu<sup>239</sup> ( $\alpha, xn$ ) excitation functions with increasing  $x$  (Fig. 4 and Appendix II). Unfortunately, as the number of neutrons emitted increases greater uncertainty in total chain yield and consequently in the determination of this number results.

The fission product distribution data for Pu<sup>239</sup> (Fig. 7) seem to be sufficiently accurate to justify some further comments. The transition from largely asymmetric to largely symmetric fission as the energy of the bombarding helium ions is increased can be clearly seen. Since fission at many degrees of excitation from 5-6 Mev up to about the energy of the incident projectile is probably taking place, depending on the stage of spallation at which the fission occurs, each of the curves can be considered to be the summation of many ranging continuously from nearly the extreme slow neutron double humped to the extreme (at least at the highest energies) single humped shapes. The transition from a double to a single "humped" final composite distribution seems to occur for helium ions with energy in the neighborhood of 40 Mev. The general features of these curves seem to be in general agreement with previous work.<sup>1,6,49,50</sup> However, recent work by Hicks and Gilbert<sup>22</sup> on the high energy deuteron induced fission of uranium

indicates the presence of two peaks in the fission product distribution curve for deuteron energies well above 40 Mev.

#### V. ACKNOWLEDGEMENTS

The authors would like to express their appreciation to Dr. J. G. Hamilton and the operating crew of the Crocker 60-inch cyclotron, and especially to the late G. Bernard Rossi, and to the Health Chemistry Group of the Radiation Laboratory for their time and aid in handling the targets. We also appreciate being able to use the absolute beta counting corrections of Hicks, Stevenson and Gilbert<sup>21,22</sup> before publication. We wish to acknowledge valuable discussions with Dr. B. G. Harvey.

This work was performed under the auspices of the U. S. Atomic Energy Commission.



## APPENDIX I

A. Target Preparation

36

Considerable experimentation was required before suitable conditions for the electrodeposition of plutonium (the only practical way to prepare uniform targets from limited quantities of target material) were determined. No previous methods for electroplating 0.2 to 1 mg of plutonium on aluminum have been reported. Electrodeposition from basic solutions<sup>51</sup> could not be used. The most successful method was patterned after the oxalate method described by Hufford and Scott<sup>52</sup>. An oxidizing (KBrO<sub>3</sub>) solution containing Pu (VI) in conc. hydrochloric acid was evaporated to dryness and the residue was redissolved in 1-2 ml. of 0.4 M ammonium oxalate. This solution was then used in a plating cell formed by a small glass tube sealed by a gasket onto the aluminum target plate. A platinum stirring disc served as the anode using  $\sim 100-200 \text{ ma/cm}^2$  at a potential  $\leq 4$  volts. Usually one such plating for  $\sim 1/2$  hour would yield 0.2-0.4 mg plutonium at  $\sim 50$  percent yield. Removal and drying of the very adherent deposit on the plate would enable further platings over the original deposit up to a 1-2 mg. Pin-hole scanning of the alpha particle emission showed the plates to be sufficiently uniform. Assays were made directly in a calibrated low geometry scintillation counter.

B. Chemical Procedure

The isolation of the fission and spallation products from the bombarded target was performed in a sequence of operations on the entire target, rather than on separate aliquots. This was done to reduce target material and cyclotron time. After the products were crudely separated from the original solution, specific chemical operations were performed to isolate each of the elements according to the procedures found in the Meinke<sup>53</sup> and the Coryell and Sugarman<sup>54</sup> compilations. The unavoidable dissolution of large (130 mg) quantities of aluminum along with the target introduced added complications. Further, the high specific activity of the plutonium isotopes required that the initial chemistry be performed in enclosed glove boxes.

Since the target material (a partially dehydrated  $\text{PuO}_2$ ) tends to become refractory the dissolution was a somewhat tedious procedure. When bromine and iodine were to be determined perchloric and hydrofluoric acid mixtures were used; otherwise, aqua regia treatment was satisfactory. After dissolution, alpha particle counting assays were made to determine the amount of plutonium remaining on the original target plate.

I, Br, Ru - Iodine, bromine, and ruthenium were removed and purified by standard distillation procedures. The aluminum target material was removed by precipitation and successive reprecipitations of all of the other carrier materials from strong  $\text{NaOH-Na}_2\text{CO}_3$  solutions in which aluminum remains dissolved.

Sr, Ba - Barium and strontium were removed by dissolving the above resulting precipitate in hydrochloric acid followed by cooling in an ice bath and precipitation of  $\text{BaCl}_2$  and  $\text{SrCl}_2$  by saturation of the solution with hydrochloric acid gas. Barium and strontium were separated by selective chromate precipitation at controlled pH's, and finally mounted as  $\text{BaCrO}_4$  and  $\text{SrCO}_3$  for counting and weighing.

Cd - Cadmium was removed on a column packed with resin Dowex A-1 ion exchange resin which, with 10-12 M  $\text{HCl}$ , does not in general hold the actinides or rare earth elements, but does retain Pu (IV). Cadmium was then removed by stripping with 0.75 M  $\text{H}_2\text{SO}_4$ , followed by antimony sulfide scavenging and final precipitation from a solution of lower acidity and mounting as cadmium sulfide for counting and weighing.

Rare earth-Actinide separation - The actinide and rare earth elements were separated from other elements by co-precipitation of the fluorides using lanthanum fluoride carrier. After dissolution in  $\text{H}_3\text{BO}_3\text{-HNO}_3$ , a hydroxide precipitate was formed, which was dissolved with  $\text{HCl}$  gas. The resulting solution was passed into a column packed with Dowex-50 ion exchange resin for a rare-earth-actinide separation.<sup>55</sup> Actinide ions are selectively eluted before rare earth ions with an eluting solution of 20 percent ethyl alcohol saturated with  $\text{HCl}$  gas.<sup>56</sup>

Ce, Eu - Cerium and europium were separated from each other by selective reduction of the europium; both cerium and europium were finally mounted as the oxalates. In some runs the column procedure recommended by Nervik<sup>57</sup> was used for separation of these rare earths from each other.

Am, Cm - The americium and curium (carrier free) HCl solution from the column packed with Dowex-50 ion exchange resin was boiled to dryness and then the two elements were separated from each other by elution with a solution containing lactate ions from a column packed with Dowex-50 cation-exchange resin.<sup>58</sup> Counting rates of a few alpha particle counts/min. were successfully separated from  $10^7$  -  $10^8$  c/m of target materials.

### C. Counting Procedures

Fission Products - These were counted using Amperex (halogenfilled) geiger counters with suitable corrections (See Sec. II - Experimental Procedures). The yields of  $\text{Sr}^{91}$  and  $\text{Cd}^{117\text{m}}$  are particularly uncertain because of the similarity of the half lives of the daughters to those of the parents ( $\text{Sr}^{91}$  and  $\text{Cd}^{117\text{m}}$ ).

Spallation Products - The americium and curium isotopes were volatilized from a hot tungsten filament in vacuum onto platinum discs. Some of the curium fractions contained up to four of the possible alpha emitters:  $\text{Cm}^{238,240,241,242}$  and tracer  $\text{Cm}^{244}$ . Alpha pulse analysis<sup>24</sup> served to resolve the alpha particles from the various isotopes. Standard alpha particle counting by argon filled ionization counters with non-selective energy amplification was also used. In the case of  $\text{Cm}^{241}$ , only  $0.96 \pm 0.07\%$  of the decay is by alpha emission,<sup>59</sup> the rest being by electron capture. Thus the yield of this nuclide was generally determined by counting the electron capture radiations; this counting efficiency (82 percent) has been determined<sup>59</sup>, by measuring the alpha particle rate of the daughter  $\text{Am}^{241}$ .

The amounts of americium isotopes,  $\text{Am}^{241}$  and tracer  $\text{Am}^{243}$  were determined by alpha pulse analysis. The  $\text{Pu}^{239}$  ( $\alpha, n$ ) product,  $\text{Am}^{242\text{m}}$  was determined by counting the alpha particles from the  $\text{Cm}^{242}$  daughter activity after a suitable growth period had elapsed. The electron capture radiation from  $\text{Am}^{240}$  was counted in a windowless proportional counter; the counting efficiency of 80-90 percent<sup>59</sup> was determined approximately by measuring the alpha disintegration rate of the daughter  $\text{Pu}^{240}$ . The yield of  $\text{Am}^{239}$  was similarly determined even more approximately; in this case a counting efficiency of 60-80 percent<sup>59</sup> was determined by measuring the alpha disintegration rate of daughter  $\text{Pu}^{239}$ . It appears that sample thinness is

fairly important for high counting efficiencies of Auger electrons (due to self absorption) which are counted in the proportional counters. This factor has led to a marked lack of reproducibility in the cases of the  $\text{Am}^{239}$  and  $\text{Am}^{240}$  counting efficiencies. Counting of x-rays is a possible solution to the problem of counting electron capture isotopes.

## APPENDIX II

### Approximate Deduction of Neutron Emission and Fission Branching Ratios from $(\alpha, xn)$ Excitation Functions

The  $(\alpha, xn)$  excitation functions (Figs. 3, 4, and 5) provide an unusual opportunity for deduction of mean neutron emission and fission branching ratios for the compound and intermediate compound nuclei involved in the reactions, including also conclusions regarding their variation with excitation energy and nuclear type. The basis for the treatment is compound nucleus formation followed by evaporation, and for this reason the  $(\alpha, n)$  reaction is not considered. The fate of each intermediate nucleus in the evaporation chain is determined by its branching ratios<sup>60</sup> (level width ratios) for neutron emission,  $\Gamma_n / \sum_i \Gamma_i$  (henceforth designated as  $G_n$ ); fission,  $\Gamma_f / \sum_r \Gamma_r$  ( $G_f$ ); and gamma ray de-excitation,  $\Gamma_\gamma / \sum_i \Gamma_i$  ( $G_\gamma$ ). The "total width",  $\sum_r \Gamma_r$ , is in principle a summation taken over all possible de-excitation modes, although products from some contributing reactions were undetectable in the present radiochemical experiments. This difficulty is minimized, however, by the fact that one process, i.e. fission, which is accounted for supplies by far the most important term. It will also be noted that each given energy of incident helium ion leads to a continuum of states and a range of excitation energies for the intermediate nuclei, depending upon the kinetic energy carried out by neutrons, so that  $\Gamma_n$  and  $\sum_i \Gamma_i$  are averages over this small energy range.

The potentially complex variation of these ratios with excitation energy and nuclear type ( $Z, A$ , odd-even character, etc.) is somewhat simplified by the fact that above 5-6 Mev essentially only neutron emission and fission compete, and below this approximate threshold energy for neutron emission and fission only the slower gamma ray emission occurs. Thus the expressions for the  $(\alpha, xn)$  cross sections of  $\text{Pu}^{239}$ .

$$\sigma(\alpha, 2n) = G_{n3} G_{n2} G_{\gamma 1} \sigma_t,$$

$$\sigma(\alpha, 3n) = G_{n3} G_{n2} G_{n1} G_{\gamma 0} \sigma_t,$$

$$\sigma(\alpha, 4n) = G_{n3} G_{n2} G_{n1} G_{n0} G_{\gamma 9} \sigma_t,$$

where subscripts 3,2,1,0, and 9 refer to  $Cm^{243}$ ,  $Cm^{242}$ ,  $Cm^{241}$ ,  $Cm^{240}$ , and  $Cm^{239}$ , respectively, are simplified for those helium ion energies leading to an excitation energy for a given product of less than 5-6 Mev, since  $G_{\gamma}$  values become unity. One helium ion energy for each excitation function where  $G_{\gamma}$  thus approaches unity is the energy corresponding to the maximum cross-section value (peak energy) as can be deduced from energy balance requirements (Q values) and energy losses by neutron kinetic energy (assuming reasonable nuclear temperatures). Hence if we restrict our considerations to cross section values at peak energies the  $G_{\gamma}$  terms drop out of the equations, and in so doing we also treat points of relative freedom from "tail" contributions (non-compound nucleus) to the cross sections.

Consider first the  $(\alpha, 2n)$  reaction in  $Pu^{238}$  and  $(\alpha, 3n)$  reaction in  $Pu^{239}$  for which  $Cm^{240}$  is the product nuclide and identical intermediate nuclei possess similar excitation energies if the respective peak energies are considered. The ratio of cross sections,

$$\frac{\sigma(\alpha, 2n)_{238}}{\sigma(\alpha, 2n)_{239}} = \frac{G_{n2} G_{n1} \sigma_t 238}{G_{n3} G_{n2} G_{n1} \sigma_t 239}$$

equals  $1/G_{n3}$  times the total cross section ratio (taken from Fig. 10). The  $G_{n3}$  value obtained, representing the neutron emission branching ratio in  $Cm^{243}$  excited to 30 Mev, is 0.30. Subtracting this number from one leaves a fission branching ratio of about 0.70 and dividing the branching ratios gives a level width ratio,  $\Gamma_f/\Gamma_n$ , of 2.3, or over two to one fission to neutron emission in  $Cm^{243}$ . Although  $Cm^{243}$  is the only nuclide which can be assigned unique branching ratios, geometric mean values over two or three nuclides can be evaluated in many cases. The ratio of the peak cross section for each  $(\alpha, xn)$  excitation function to the total reaction cross section for the appropriate helium ion energy (from Fig. 10) equals the product of a number of neutron emission branching ratios, such that mean values are obtained by extracting the square root of the ratio for an  $(\alpha, 2n)$  peak, the cube root for an  $(\alpha, 3n)$  peak, and a fourth root for an  $(\alpha, 4n)$  peak.

For example, the calculation of

$$G_n(\text{mean}) = \sqrt[3]{G_{n3} G_{n2} G_{n1}} = \sqrt[3]{\sigma(\alpha, 3n) / \sigma_t}$$

gives the mean value of the neutron emission branching ratios for Cm<sup>243</sup> excited to 30 Mev, Cm<sup>242</sup> excited to 22 Mev, and Cm<sup>241</sup> excited to 12 Mev and, putting in the proper numerical values, equals 0.20. Calculations have been performed for all possible cases and the results are tabulated in Table IV.

Table IV  
Neutron Emission Branching Ratios ( $G_n$ ) and Fission to Neutron Emission Ratios ( $\Gamma_f / \Gamma_n$ ) for Curium Isotopes

Target Nuclide	Reaction	Product Nuclide	Intermediate Nuclides	$G_n$ , Mean	$\Gamma_f / \Gamma_n$ , Mean
Pu <sup>238</sup>	( $\alpha, 2n$ )	Cm <sup>240</sup>	Cm <sup>242, 241</sup>	0.16	5.2
Pu <sup>238</sup>	( $\alpha, 4n$ )	Cm <sup>238</sup>	Cm <sup>242, 241, 240, 239</sup>	0.12	7.3
Pu <sup>239</sup>	( $\alpha, 2n$ )	Cm <sup>241</sup>	Cm <sup>243, 242</sup>	0.24	3.2
Pu <sup>239</sup>	( $\alpha, 3n$ )	Cm <sup>240</sup>	Cm <sup>243, 242, 241</sup>	0.20	4.0
Pu <sup>239</sup>	( $\alpha, 4n$ )	Cm <sup>239</sup>	Cm <sup>243, 242, 241, 240</sup>	0.16	5.4
Pu <sup>242</sup>	( $\alpha, 2n$ )	Cm <sup>244</sup>	Cm <sup>246, 245</sup>	0.66	0.52
Pu <sup>242</sup>	( $\alpha, 4n$ )	Cm <sup>242</sup>	Cm <sup>246, 245, 244, 243</sup>	0.30	2.3

It is seen that the  $G_n$  value of 0.30 for Cm<sup>243</sup> is the same order of magnitude as the mean value of 0.20 for  $G_{n3}$ ,  $G_{n2}$ , and  $G_{n1}$  from  $\sigma(\alpha, 3n)_{239}$  and  $\sigma_{t239}$  alone and also the mean value of 0.16 for  $G_{n2}$  and  $G_{n1}$  from  $\sigma(\alpha, 2n)_{238}$  and  $\sigma_{t238}$  alone. As a first approximation then, comparable numbers of Cm<sup>242</sup> and Cm<sup>241</sup> nuclei to Cm<sup>243</sup> nuclei are going into fission; that is, fission is occurring prominently all along the evaporation path. The 8-9 Mev higher excitation energy of Cm<sup>243</sup>, therefore, is not decisive one way or the other, for fission liability or stability.

It is difficult to assess exactly how much of the variation in  $G_n$  and  $\Gamma_f / \Gamma_n$  is due to differences in excitation energy and how much to differences in A and odd-even character. The uncertainties of at least  $\pm 25$  percent that must be attached to the numbers is a further complicating factor. In addition, it is probable that a certain amount of the lowering of successive ( $\alpha, xn$ ) peaks may be due to the fact that as the energy of the incident alpha particle increases relatively more knock-on or direct

interaction reactions<sup>38,61</sup> take place. Alpha particles are thereby removed that might have formed compound nuclei and which in turn would have lead preponderantly to  $(\alpha, 3n)$  and  $(\alpha, 4n)$  reactions (at the upper range of energies under consideration).

Apart from these difficulties, nevertheless, two observations that can be made from the information in Table III are that fission is occurring over a range of nuclides and that there is a transition in Gn from about 0.2 to 0.6 from the lightest to heaviest curium isotopes. It appears that the indicated stability towards fission associated with the larger mass numbers might explain the entire variation in Table III.

The relative  $(\alpha, 2n)$  and  $(\alpha, 4n)$  reactions  $\text{Pu}^{238}$  and  $\text{Pu}^{242}$  are an interesting consequence of the step-wise fission competition picture. The ratio of the  $(\alpha, 2n)$  maximum cross section values is about 6.9 (103 mb for  $\text{Pu}^{242}$  divided by 15 mb for  $\text{Pu}^{238}$ ) whereas the ratio of the  $(\alpha, 4n)$  maximum cross section values is about 35 (9 mb for  $\text{Pu}^{242}$  divided by 0.26 mb for  $\text{Pu}^{238}$ ). At first one might have expected equal ratios, but consideration of the fact that the fission reaction has had two chances, so to speak, to interrupt the chain leading to the  $(\alpha, 2n)$  reaction products and four chances in the case of the  $(\alpha, 4n)$  reaction necessitates a different comparison. If we take the square root of the ratio of the  $(\alpha, 2n)$  cross sections ( $\sqrt{6.9} = 2.6$ ) and the fourth root of the ratio of the  $(\alpha, 4n)$  cross sections ( $\sqrt[4]{35} = 2.4$ ) to obtain quantities related to the mean neutron emission branching ratios, roughly equal numbers result. This interesting outcome also shows that the variation in  $G_f$  or  $\Gamma_f/\Gamma_n$  over the four nuclides involved in the  $(\alpha, 2n)$  and  $(\alpha, 4n)$  reactions is about the same for  $\text{Pu}^{238}$  and  $\text{Pu}^{242}$  target nuclei.

## REFERENCES

1. For references see, for example, W. J. Whitehouse, *Progr. Nuc. Phys.* 2, 120 (1952); W. E. Nervick and G. T. Seaborg, *Phys. Rev.* 97, 1092 (1955); R. L. Folger, P. C. Stevenson, and G. T. Seaborg, *Phys. Rev.* 98, 107 (1955).
2. See appendix of Ref. 6 for a summary of references to work done previous to 1950. For a summary of more recent work see O. C. Anders and W. W. Meinke, American Documentation Institute, Washington 25, D. C., U. S. A.
3. Ph.D. thesis of K. Street, Jr., University of California, June 1949 (also published as University of California Radiation Laboratory Unclassified Report UCRL-301 (March 1949).
4. Ph.D. thesis of W. W. Meinke, University of California, January 1950 (also published as University of California Radiation Laboratory Unclassified Report UCRL-483 (November 1949).
5. W. W. Meinke, G. C. Wick, and G. T. Seaborg, University of California Radiation Laboratory Declassified Report UCRL-868 (September 1950); *J. Inorg. Nuc. Chem.*, in press.
6. H. A. Tewes and R. A. James, *Phys. Rev.* 88, 860 (1952); H. A. Tewes, *Phys. Rev.* 98, 25 (1955).
7. G. H. McCormick and B. L. Cohen, *Phys. Rev.* 96, 722 (1954); B. L. Cohen, *Phys. Rev.* 98, 49 (1955).
8. M. Lindner and R. N. Osborne, University of California Radiation Laboratory Unclassified Report UCRL-4626 (December 1955); *Phys. Rev.*, in press.
9. R. H. Goeckermann and I. Perlman, *Phys. Rev.* 76, 628 (1949).
10. P. Kruger and N. Sugarman, *Phys. Rev.* 99, 1459 (1955).
11. A. W. Fairhall, private communications of report "Fission of Bismuth with 15 and 22 Mev Deuterons" (January 1956); *Phys. Rev.*, in press.
12. A. P. Vinogradov, I. P. Alimarin, V. I. Baranova, A. K. Lavrukhima, T. V. Baranova, F. I. Pavlotskaya, A. A. Bragina, and I. V. Yakovlev, Report of the Moscow Conference of the Academy of Science U.S.S.R. on the Peaceful Applications of Atomic Energy, Division of Chemical Sciences. (July 1-5, 1955).



13. J. A. Jungerman, Phys. Rev. 79, 632 (1950); H. M. Steiner and J. A. Jungerman, Phys. Rev. 101, 807 (1956).
14. E. L. Kelley and E. Segrè, Phys. Rev. 75, 999 (1949).
15. Ph.D. thesis of W. John, Jr., University of California, 1955 (also published as University of California Radiation Laboratory Unclassified Report UCRL-3093 (August 1955)).
16. A. S. Newton, Phys. Rev. 75, 17 (1949).
17. A. Ghiorso, B. G. Harvey, G. R. Choppin, S. G. Thompson, and G. T. Seaborg, Phys. Rev. 98, 1518 (1955).
18. The range-energy curves of W. A. Aron, B. G. Hoffman, and F. C. Williams are used. U. S. Atomic Energy Commission Unclassified Document AECU-663 (May 1951).
19. B. P. Burt, Nucleonics 5, No. 2, 28 (1949).
20. W. Nervick and P. C. Stevenson, Nucleonics 10, No. 3, 18 (1952).
21. H. G. Hicks, P. C. Stevenson, R. S. Gilbert, and W. H. Hutchin, Phys. Rev. 100, 1284 (1955).
22. H. G. Hicks and R. S. Gilbert, Phys. Rev. 100, 1286 (1955).
23. W. M. Gibson, W. H. Wade, R. A. Glass, and G. T. Seaborg, unpublished data.
24. A. Ghiorso, A. H. Jaffey, H. P. Robinson, and B. B. Weissbourd, The Transuranium Elements: Research Papers (McGraw-Hill Book Company, Inc., New York, 1949), National Nuclear Energy Series, Plutonium Project Record, Vol. 14B, paper 16.8.
25. For example, electron capture disintegration rates to be compared with counting rates in order to establish counting efficiencies have been calculated from the growth of alpha-active daughters for  $\text{Np}^{234}$ ,  $\text{Am}^{238}$ ,  $\text{Am}^{239}$ ,  $\text{Am}^{240}$ , and  $\text{Cm}^{241}$ .
26. We are indebted to Dr. Stanley G. Thompson for supplying these tracers.
27. G. B. Rossi and W. B. Jones, private communication.
28. Cross sections for helium ions on  $\text{Np}^{237}$  have been determined by W. M. Gibson, R. A. Glass, and G. T. Seaborg, unpublished data.
29. M.S. Thesis of S. E. Ritsema, University of California, January 1956 (also published as University of California Radiation Laboratory Unclassified Report UCRL-3266 (January 1956)).

30. PhD thesis of H. D. Sharma, University of California, 1951 (also published as University of California Radiation Laboratory Unclassified Report UCRL-1265 (May 1951).
31. J. M. Blatt and V. F. Weisskopf, Theoretical Nuclear Physics, John Wiley and Sons, Inc., New York (1952), pp. 352-3.
32. Ph.D. thesis of E. L. Kelley, University of California, January 1951 (also published as University of California Radiation Laboratory Unclassified Report UCRL-1044 (December 1950).
33. N. Bohr and J. A. Wheeler, Phys. Rev. 56, 426 (1939).
34. J. R. Huizenga, W. M. Manning, and G. T. Seaborg, (McGraw-Hill Book Company, Inc., New York, 1954) National Nuclear Energy Series, Plutonium Project Record, Vol. 14A, Chap. 20.
35. W. J. Whitehouse, Progr. Nuc. Phys. 2, 120 (1952).
36. W. J. Whitehouse and W. Galbraith, Nature 169, 494 (1952).
37. G. T. Seaborg, Phys. Rev. 85, 157 (1952).
38. R. Nakasima and K. Kikuchi, Prog. Theor. Phys. 14, 126 (1955).
39. S. N. Ghoshal, Phys. Rev. 80, 939 (1950).
40. D. H. Templeton, J. J. Howland, and I. Perlman, Phys. Rev. 72, 758 and 766 (1947).
41. F. N. Spiess, Phys. Rev. 94, 1292 (1954).
42. T. D. Thomas, R. A. Glass, and G. T. Seaborg (unpublished data).
43. A. Chetham-Strode, Jr., G. R. Choppin, and B. G. Harvey, Phys. Rev. 102, 747 (1956)
44. B. G. Harvey, A. Chetham-Strode, Jr., A. Ghiorso, G. R. Choppin, and S. G. Thompson, unpublished data.
45. W. H. Wade, J. Gonzalez-Vidal, R. A. Glass, and G. T. Seaborg, unpublished data.
46. The product observed would have been  $\text{Cm}^{244}$ , the product also of the  $(\alpha, 2n)$  reaction.
47. K. F. Chackett, J. H. Fremlin, and D. Walker, Phil. Mag. 45, 173 (1954)
48. B. G. Harvey, Report of the Symposium on Nuclear and Radiochemistry of the Chemical Institute of Canada, Physical Chemistry Subject Division, McGill University, Montreal, Canada (September 7-9, 1955).
49. W. H. Jones, A. Timnick, J. H. Paehler, and T. H. Handley, Phys. Rev. 99, 184 (1955).

50. L. Katz, T. M. Kavanagh, A. G. W. Cameron, E. C. Bailey, and J. W. T. Spinks, *Phys. Rev.* 99, 98 (1955).
51. H. W. Miller and R. J. Brouns, *Anal. Chem.* 24, 536 (1952).
52. D. L. Hufford and B. F. Scott, The Transuranium Elements: Research Papers (McGraw-Hill Book Company, Inc., New York (1949) National Nuclear Energy Series, Plutonium Project Record Vol. 14B, p. 1149.
53. W. W. Meinke, University of California Radiation Laboratory Unclassified Report UCRL-432, Addenda 1 and 2 (August 1949).
54. C. D. Coryell and M. Sugarman, Radiochemical Studies: The Fission Products (McGraw-Hill Book Company, Inc., New York 1951), National Nuclear Energy Series, Plutonium Project Record, Volume 9.
55. K. Street, Jr., and G. T. Seaborg, *J. Am. Chem. Soc.* 72, 2790 (1950).
56. S. G. Thompson, B. G. Harvey, G. R. Choppin, and G. T. Seaborg, *J. Am. Chem. Soc.* 76, 6229 (1954).
57. W. E. Nervick, *J. Phys. Chem.* 59, 690 (1950).
58. R. A. Glass, *J. Am. Chem. Soc.* 77, 807 (1955).
59. R. A. Glass, W. Gibson, and J. W. Cobble, unpublished data.
60. The terminology employed follows that of Blatt and Weisskopf (Ref. 32) and P. Morrison, Experimental Nuclear Physics (John Wiley and Sons, Inc., New York, 1953) Vol. II, part VI.
61. R. E. Bell, *Phys. Rev.* 95, 651 (1954); R. E. Bell and H. M. Skarsgard, paper presented at the Toronto Meeting of the Royal Society of Canada (June 6-8, 1955), Atomic Energy of Canada, Limited Report AECL-221.

I-III AND

1-46

THIS PAGE  
WAS INTENTIONALLY  
LEFT BLANK